nature geoscience
SUPPLEMENTARY INFORMATION
DOI: 10.1038/NGEO2700

Long-lived connection between southern Siberia and northern Laurentia in the Proterozoic

R.E. Ernst, M.A. Hamilton, U. Söderlund, J.A. Hanes, D.P. Gladkochub, A.V. Okrugin, T. Kolotilina, A.S. Mekhonoshin, W. Bleeker, A.N. LeCheminant, K.L. Buchan, K.R. Chamberlain, A.N. Didenko

Table of Contents

S1 Reconstructions of Siberia and Laurentia from the literature

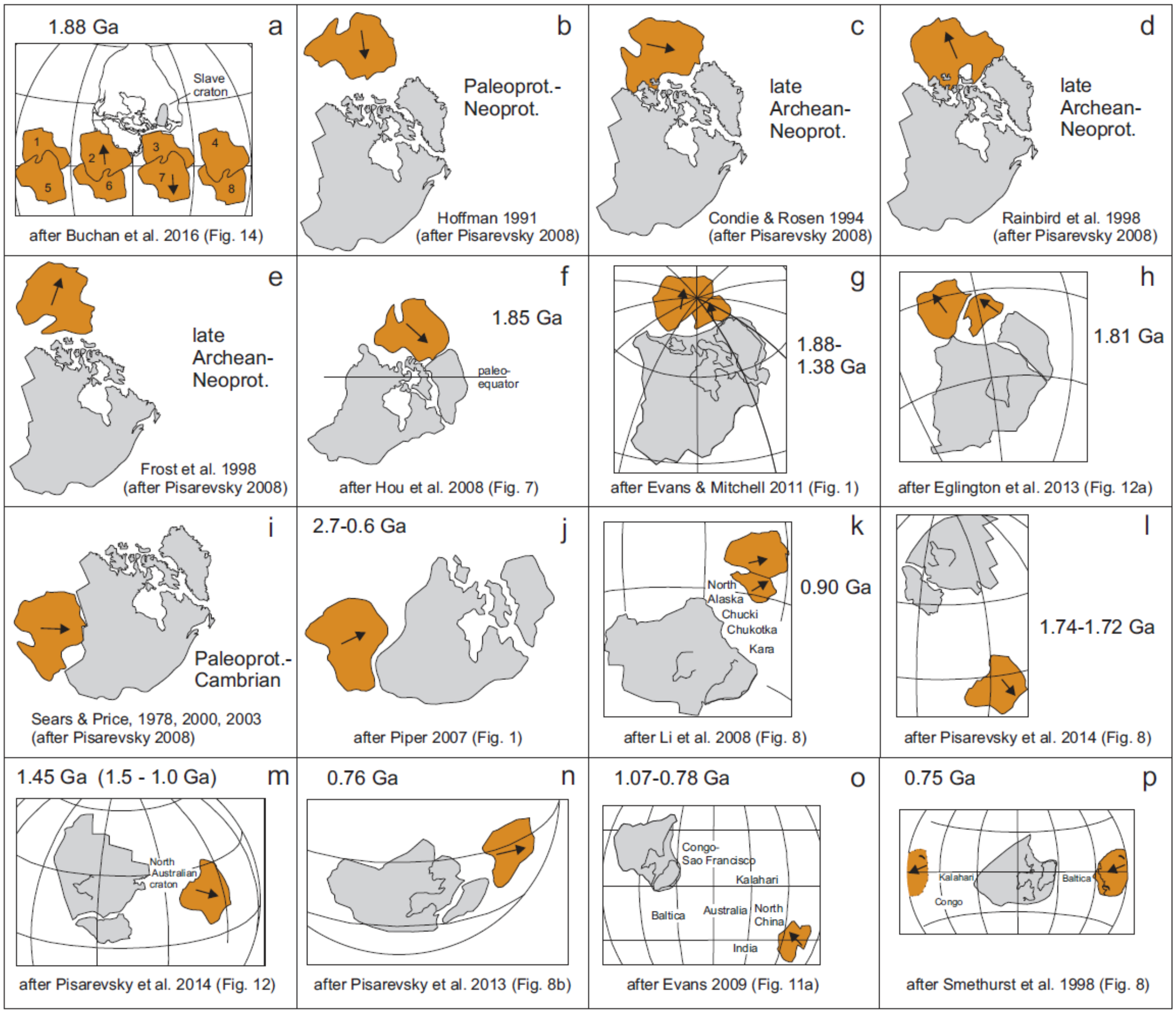

Figure S1: *Selected published reconstructions of Siberia and Laurentia based on geology and/or paleomagnetism. Siberia is shown in orange-brown, and Laurentia (including Greenland) or the Laurentian precursor Slave craton is shown in grey. For clarity an arrow indicating present-day north has been added to Siberia or its components.*

As illustrated in Figure S1, there are a wide variety of published reconstructions of Siberia and Laurentia (or their pre-1.8 Ga components). In some cases, they are thought to be valid from the Paleoproterozoic (or even late Archean) to the Neoproterozoic (or Early Cambrian). In other cases, they are restricted to a narrower time range as indicated on the figure. The reconstructions are based on geological and/or paleomagnetic constraints.

Paleomagnetism has the potential to provide a unique reconstruction. However, this requires apparent polar wander paths (APWPs) for each craton that are derived from key paleomagnetic poles (Buchan 2014), that is, paleopoles that are well-constrained and precisely dated. A paleopole is precisely dated if (a) the rock unit from which it is derived has a precise age (usually from U-Pb geochronology) and (b) the paleopole has been demonstrated primary. Currently there are a number of Paleoproterozoic – Neoproterozoic key paleopoles for Laurentia (and its Slave craton precursor). However, precisely dated key poles for this period are not yet available for Siberia or its precursors except at 1.88 Ga (Didenko et al. 2009) as discussed by Buchan (2014). Therefore, the only key pole comparison that is available is at 1.88 Ga (Buchan et al. 2016) (Fig. S1a). It permits a Siberia –Slave craton fit, but because it is a based on a single key pole match, it is insufficient to define a unique fit (as discussed below). Other paleomagnetic reconstructions have relied on poorly dated non-key paleopoles from Siberia, many of whose ages are open to interpretation, resulting in variety of divergent reconstructions.

Siberia is often placed adjacent to the northern margin of Laurentia, with the present-day northern Siberia margin facing in a variety of different directions with respect to northern Laurentia (e.g., Hoffman 1991, Condie and Rosen 1994, Rainbird et al. 1998, Frost et al. 1998, Hou et al. 2008; Evans and Mitchell 2011; Eglington et al. 2013) (Fig. S1b-h). In some cases, these reconstructions are based mainly on geological considerations, including the matching of Paleoproterozoic orogenic belts between the two cratons (e.g., Hoffman 1991, Condie and Rosen 1994, Rainbird et al. 1998, Frost et al. 1998, Hou et al. 2008) (Fig S1b-f). On the other hand, paleomagnetic reconstructions by Buchan et al. (2001) (not shown in Fig. S1), Evans and Mitchell (2011) (Fig. S1g) and Zhang et al. (2012) (not shown in Fig. S1) locate Siberia close to northern Laurentia with southern Siberia facing the Laurentia margin. The Buchan et al. (2011) fit was based on a single 1.50–1.45 Ga non-key pole comparison, whereas Evans and Mitchell (2011) used a broader range of non-key Siberia poles between ca. 1.88 and 1.38 Ga. Roughly similar reconstructions by Eglington et al. (2013) (Fig. S1h) and Pehrsson et al. (2015) (not shown in Fig. S1) are based on published paleomagnetic reconstructions integrated with geological and geochronological constraints using the database system developed for International Geoscience Programme (IGCP) Project 509 (e.g. Eglington et al. 2013).

Siberia has also been placed adjacent to the western margin of Laurentia with present-day northern Siberia facing western Laurentia. Such reconstructions have been based mainly on geological constraints (Sears and Price 1978, 2003), detrital zircon studies (MacLean et al. 2009) and paleomagnetism (Piper 2007). Piper utilized a very broad range of paleopoles, many of which are very poorly dated, a methodology which has been criticized as unreliable (Meert and Torsvik, 2004; Li et al. 2009).

Some paleomagnetic reconstructions of the Mesoproterozoic-Neoproterozoic supercontinent Rodinia locate Siberia and Laurentia at a considerable distance from one another with cratonic blocks or smaller terranes in between. For example, Li et al. (2008) place Siberia ~1500 km to the northwest of Laurentia with North Alaska and Chuki terranes in between (Fig. S1k). Pisarevsky et al. (2014) locate Siberia ~2500 km from northwestern Laurentia at 1.74-1.72 Ga (Fig. S1l), and somewhat closer at ca. 1.50-1.00 Ga (Fig.S1m). The latter is broadly similar to Li et al. (2008), without identifying the intervening cratonic blocks. Pisarevsky et al. (2013) indicate that Siberia then moved close to northeastern Laurentia (Greenland) by 760 Ma (Fig S1n). Evans (2009) locates Siberia ~3000 km from northeast Laurentia on opposite sides of Rodinia with several cratons in between (Fig. S1o). Smethurst et al. (1998) locates Siberia ~3000 km from Greenland with Baltica in between (Fig. S1p) or alternatively off southern Laurentia with Kalahari between (Fig. S1p).

As noted above, the only Proterozoic key paleomagnetic pole comparison available for Siberia and Laurentia or their precursors is at ca. 1.88 Ga, although it does not provide a unique fit and is only valid at that time (Buchan et al. 2016) (Fig. S1a). In this figure, the Slave craton is placed in one hemisphere at a paleolatitude and azimuthal orientation defined by the paleomagnetic data, but at an arbitrary paleolongitude. The paleomagnetic data establish the paleolatitude and orientation of Siberia, but it is permitted to occupy any paleolongitude (which is not constrained by the paleomagnetic data), and is shown in either hemisphere (because of an ambiguity in the relative magnetic polarity of the Siberia and Slave paleopoles). Siberia position 3 is similar to the position of Hoffman (1991) (Fig. S1b). Position 7 is similar to that of Rainbird et al. (1998) (Fig. S1d) or Evans and Mitchell (2011) (Fig. S1g), although a little farther from the Laurentia margin. Position 8 is similar to that of Li et al. (2008) (Fig. S1k) and the 1500-1000 Ma position of Pisarevsky et al. (2014) (Fig. S1m).

The Siberia-Laurentia reconstruction, based on the Large Igneous Province (LIP) record, that is discussed in the present paper (Fig. 2), in which southern Siberia faces northern Laurentia or its Slave-Rae precursor, can be compared with the reconstructions discussed above. It is broadly similar to the reconstructions of Rainbird et al. (1998) (Fig. S1d), Buchan et al. (2001) (not in Fig. S1), Evans and Mitchell (2011) (Fig. S1g), Eglington et al. (2013) (Fig. S1h) and (Buchan et al. 2016) (position 7 of Fig. S1a).

S2 Large Igneous Province summary

Large Igneous Provinces (LIPs) represent large volume (>0.1 Mkm^3; frequently above >1 Mkm^3), mainly mafic (-ultramafic) magmatic events of intraplate affinity, that occur in both continental and oceanic settings. They are typically of short duration (<5 myr or even less than 1 myr), or can consist of multiple short pulses over a maximum of a few 10s of m.y. (Ernst, 2014 and references therein). They comprise volcanic packages (flood basalts), and a plumbing system of dykes, sills and layered intrusions, and magmatic underplating at the base of the crust. In the Phanerozoic they are dominated by flood basalts, in the Proterozoic by the exposed plumbing systems (dykes, sills and layered intrusions) and in the Archean by both continental flood basalts and komatiite-tholeiitic greenstone belts. They can also be associated with silicic magmatism, carbonatites and kimberlites. LIP events are linked with continental breakup, global climate change including extinction events, and represent significant reservoirs of energy and metals that can either drive or contribute to a variety of metallogenic systems (particularly related to Ni-Cu-PGEs) (Ernst and Jowitt 2013). In addition, LIPs can also affect hydrocarbon and aquifer systems (Ernst 2014). LIPs occur at an average rate of one every 20-30 myr back to at least 2.5 Ga. The number and size of LIPs that have been identified is increasing through U-Pb dating (e.g. through the Industry supported LIPs-Resource Exploration project, www.supercontinent.org) where >220 U-Pb baddeleyite and zircon ages have been obtained from units around the world (Ernst et al. 2013).

The successful application of the LIP matching method in the present study to link southern Siberia and northern Laurentia, suggests this technique should be more widely applied as a complementary reconstruction tool to the traditional paleomagnetic methods.

S3 Geochronology (U-Pb and Ar-Ar) for units in southern Siberia and northern Laurentia

S3-1 OVERVIEW

Background information is provided on our U-Pb dating of the following units: 1) two layered intrusions belonging to the 725 Ma Irkutsk Large Igneous Province (LIP) in southern Siberia, 2) two dolerites of age ca. 1350 Ma, a dyke in southern Siberia and a sill in northern Laurentia, 3) a 1640 Ma sill from the Biryusa block in southern Siberia, 4) two dolerite dykes in southern Siberia belonging to 1750 Ma Timpton LIP and 5) two dolerite dykes belonging to the 1870 Ma Kalaro-Nimnyrsky LIP of southern Siberia.

In addition, Ar-Ar geochronology (a total of 18 biotite and amphibole plateau dates) are presented for four dykes of the ca. 1750 Ma Timpton LIP and for two dykes of the 1870 Ma Kalaro-Nimnyrsky LIP.

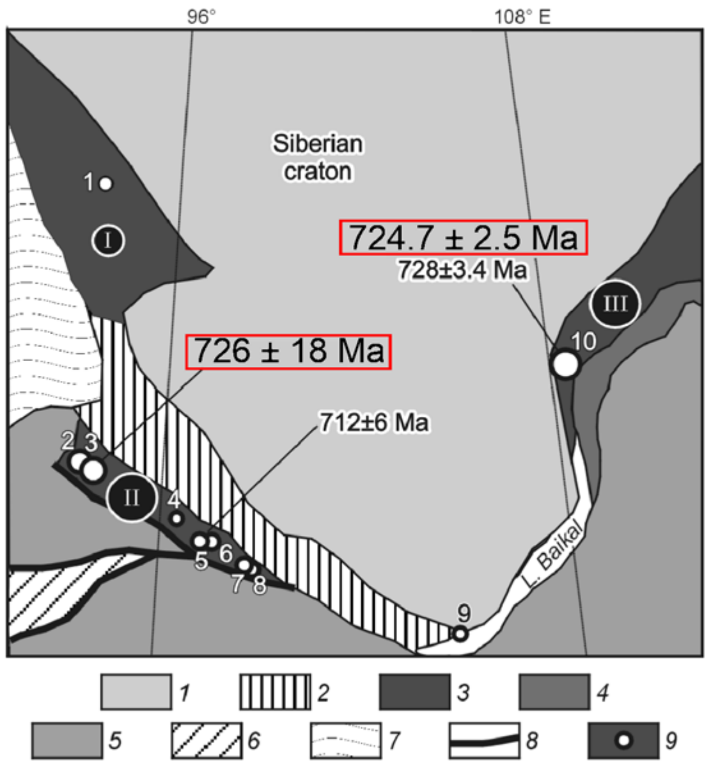

Figure S2: *Distribution of mafic-ultramafic intrusions of the East Siberian metallogenic province (modified after Figure 1 in Polyakov et al., 2013) interpreted to belong to the ca. 720 Ma Irkutsk LIP (see discussion in main text). 1 = portion of Siberian craton covered by undeformed Phanerozoic sediments; 2 = Precambrian basement exposures of the Siberian craton; 3–7 = deformed areas: 3 = Riphean; 4 = Riphean–Vendian; 5 = Early Caledonian; 6 = Late Caledonian; 7 = cover of the West Siberian Plate; 8 = suture zones; 9 = mafic-ultramafic intrusions hosting PGE– Cu–Ni deposits and ore occurrences: Number **3** = the **Verkhnii (Upper) Kingash** intrusion, dated by the U-Pb baddeleyite method (Section S3-2.2). Number **10** = the **Yoko-Dovyren (Dovyren)** intrusion, dated by U-Pb baddeleyite (Section S3-2.1) and zircon (Ariskin et al. 2013). The Tartai intrusion (number 5) is also dated by U-Pb zircon (Polyakov et al., 2013; see discussion in text). The other numbered mafic-ultramafic intrusions are: 1 = Shumikha, 2 = Kingash, 4 = Golumbei, 6 = Ognit, 7 = Zhelos, 8 = Tokty-Oi, and 9 = Malyi Zadoi. I = Yenisei Ridge; II = Sayan zone (Kan and Alkhadyr terranes); III = Baikal–Patom pericratonal trough.*

S3-2 725 MA IRKUTSK LIP, IRKUTSK PROMONTORY, SOUTHERN SIBERIA

Here we present U-Pb baddeleyite ages for both the Dovyren and Verkhnii (Upper) Kingash intrusions. Although our provisional ages for the Dovyren and Upper Kingash intrusions were mentioned in Ernst and Hamilton (2009), Ernst et al. (2012, 2014) and Polyakov et al. (2013), the analytical details and full isotopic data and plots are presented here for the first time.

S3-2.1 Dovyren mafic-ultramafic intrusion

Sample number: *143/1*
Location: *56.3114° N, 109.8422° E*
U-Pb age: *724.7 ± 2.5 Ma (5 fractions) ID-TIMS baddeleyite*
Mineral separation: *M.A. Hamilton*
Geochronology: *M.A. Hamilton*

A U-Pb baddeleyite age was determined for the Dovyren (Yoko Dovyren) intrusion (point 10 in Fig. S2), and a second U-Pb zircon age (728±3 Ma) from Ariskin et al. (2013) is also listed. This sample, from Grushevidnoye Lake, is a gabbro pegmatite with sulfide mineralization from the middle part of the Gabbro Norite Horizon. The sample was collected by Alexay Lygin, provided to us by BHP Billiton, and was processed and dated by ID-TIMS at the University of Toronto. A modest amount of fresh to somewhat dull baddeleyite was recovered, and an upper intercept age of 724.7 ± 2.5 Ma was obtained based on five variably discordant fractions (Fig. S3, Table S1). A correlation between degree of discordance and model Th/U ratios suggests that some of the discordance could be related to alteration consisting of fine, thin zircon coatings on baddeleyite (Söderlund et al. 2013). The lower intercept age for the regression broadly implies a Mesozoic Pb-loss event (~200 Ma).

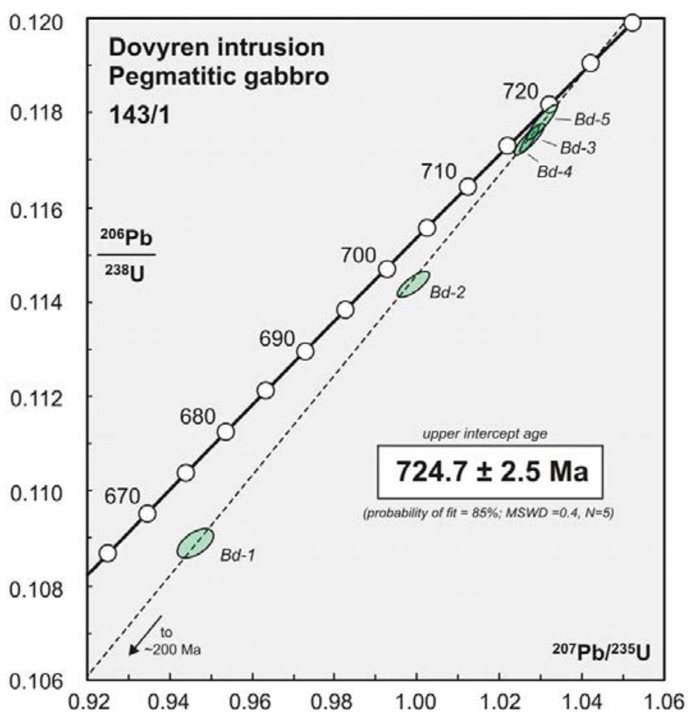

Figure S3: *Concordia diagram with U-Pb baddeleyite age for Dovyren intrusion.*

S3-2.2 Upper Kingash mafic-ultramafic intrusion

Sample number: *C-123*
Location: *54.86083° N; 95.4925° E*
U-Pb age: *726 ±18 Ma (4 fractions) ID-TIMS baddeleyite*
Mineral separation: *U. Söderlund*
Geochronology: *M.A. Hamilton*

A sample of the Upper Kingash mafic-ultramafic intrusion (point 3 in Fig. S2), located in the Kan belt, southern Siberia, was obtained from drillhole C-123, from a depth of 168.2 m - 169.2 m and provided to us by BHP Billiton. The sample represents an upper, differentiated gabbroic portion of the intrusion, and was processed to separate baddeleyite at Lund U. using the methods of Söderlund and Johansson (2002), while the dissolutions and isotopic measurements were made at the University of Toronto.

Only seven very small baddeleyite grains (max. ~15 microns) were recovered; these were subsequently analyzed in four fractions consisting of one single grain fraction and three two-grain fractions (Fig. S4). Fraction Bd-B yielded the highest Pb/Pb and U/Pb ages, overlaps concordia, and represents a minimum age for the intrusion (206/238 age = 712 Ma, 207/206 age = 718 Ma). The distribution of the data, along and close to Concordia, implies that the baddeleyites are likely affected by a non-zero-aged secondary Pb-loss event.

The flanking portions of the southern Siberian craton in the Irkutsk promontory region are known to have been affected by either Late Neoproterozoic (Vendian) deformation and metamorphism, or early Paleozoic metamorphism (late Cambrian?), probably related to docking of microterranes. This is chiefly reflected in Ar-Ar ages for amphiboles and biotites (see Turkina et al. 2007). The Kingash intrusion is also described as being cut by plagiogranite veins, which could also be related to such an overprinting event. Therefore, likely candidate ages for a younger isotopic disturbance could be roughly 590-550 Ma, or ~490 Ma, though Turkina et al. (2007) suggest that the latter age may have local significance. If secondary Pb-loss is anchored at about 490 Ma, then the upper intercept age for the Upper Kingash data (through all four fractions) is 726 ± 18 Ma (Fig. S4, Table S1). Although this age is not particularly precise, we interpret it to be reasonably accurate.

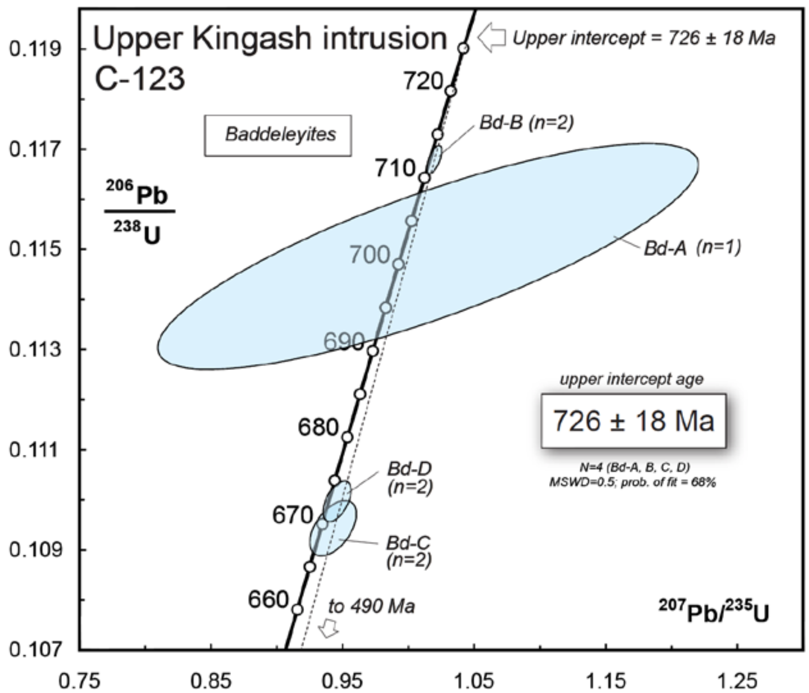

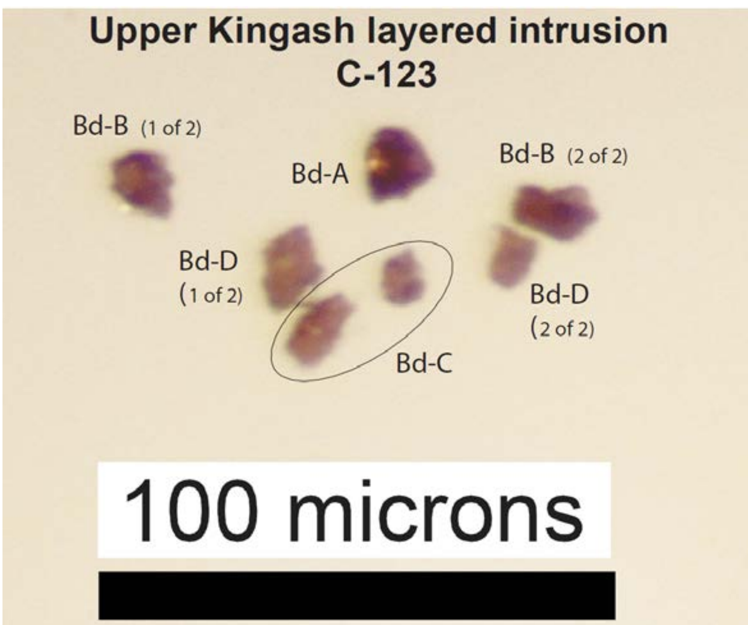

Figure S4: *Concordia diagram showing ID-TIMS U-Pb baddeleyite age for Upper Kingash intrusion. Note the very small size of the recovered baddeleyite grains and resultant fractions.*

Table S1: *Baddeleyite U-Pb isotopic data for gabbroic pegmatite and gabbro of the Dovyren and Upper Kingash layered intrusions, respectively, southern Siberian craton*

Table S1. *Baddeleyite U-Pb isotopic data for gabbroic pegmatite and gabbro of the Dovyren and Upper Kingash layered intrusions, respectively, southern Siberian craton.*

Fraction	No. grains	Weight (µg)	U (ppm)	Pb^{T} (pg)	Pb_{C} (pg)	Th/U	$^{206}Pb/^{204}Pb$	$^{206}Pb/^{238}U$	± 2σ	$^{207}Pb/^{235}U$	± 2σ	$^{207}Pb/^{206}Pb$	± 2σ	Ages (Ma) $^{206}Pb/^{238}U$	± 2σ	$^{207}Pb/^{235}U$	± 2σ	$^{207}Pb/^{206}Pb$	± 2σ	Disc. (%)
Sample **143-1** (gabbroic pegmatite, Dovyren intrusion)																				
Bd-1	5	0.5	736	6.74	1.88	0.387	922	0.108888	0.000261	0.94582	0.00363	0.062999	0.000202	666.3	1.5	675.9	1.9	708.2	6.8	6.2
Bd-2	11	0.4	845	6.69	1.27	0.114	4616	0.114359	0.000223	0.99868	0.00321	0.063335	0.000134	698.0	1.3	703.1	1.6	719.5	4.5	3.2
Bd-3	10	0.1	605	6.48	0.83	0.033	4091	0.117422	0.000228	1.02694	0.00182	0.063431	0.000057	715.7	1.3	717.4	0.9	722.7	1.9	1.0
Bd-4	8	0.2	379	5.14	0.48	0.091	5172	0.117419	0.000276	1.02691	0.00294	0.063430	0.000090	715.7	1.6	717.4	1.5	722.7	3.0	1.0
Bd-5	6	0.2	351	5.07	0.27	0.034	3725	0.117776	0.000303	1.02992	0.00301	0.063422	0.000078	717.8	1.7	718.9	1.5	722.4	2.6	0.7
Sample **C-123** (gabbro, Upper Kingash intrusion)																				
Bd-1	1	0.1	51	2.03	1.08	0.031	77	0.114843	0.001855	1.01451	0.16892	0.064069	0.009908	700.8	10.7	711.1	86.8	743.9	343.9	6.1
Bd-2	2	0.3	631	13.48	0.33	0.039	2862	0.116786	0.000233	1.01926	0.00442	0.063299	0.000216	712.0	1.3	713.5	2.2	718.3	7.3	0.9
Bd-3	2	0.2	144	2.86	0.29	0.035	712	0.109370	0.000457	0.94193	0.01435	0.062462	0.000848	669.1	2.7	673.9	7.5	690.0	29.1	3.2
Bd-4	2	0.2	244	4.93	0.28	0.031	1239	0.109905	0.000332	0.94188	0.00875	0.062155	0.000504	672.2	1.9	673.9	4.6	679.4	17.4	1.1

Notes:
All analyzed fractions represent best quality, fresh grains of pale to medium-brown blades and blade fragments of baddeleyite.
Abbreviations: brn - brown; bl- blade; frags - fragments
PbT is total amount (in picograms) of Pb.
PbC is total measured common Pb (in picograms) assuming the isotopic composition of laboratory blank: 206/204 - 18.221; 207/204 - 15.612; 208/204 - 39.360 (errors of 2%).
Pb/U atomic ratios are corrected for spike, fractionation, blank, and, where necessary, initial common Pb; 206Pb/204Pb is corrected for spike and fractionation.
Th/U is model value calculated from radiogenic 208Pb/206Pb ratio and 207Pb/206Pb age, assuming concordance.
Disc. (%) - per cent discordance for the given 207Pb/206Pb age.
Uranium decay constants are from Jaffey et al. (1971).

S3-3 1260 MA MAGMATISM OF IRKUTSK PROMONTORY, SOUTHERN SIBERIA

S3-3.1 Srednecheremshansky mafic-ultramafic dyke

Sample number: *90-22*
Location: *52.22361° N, 102.94743° E*
Dyke trend, dip, thickness: *NNE, dipping 75° -80° W, ~200 m.*
U-Pb age: *1258 ± 5 Ma (U-Pb ID-TIMS on baddeleyite)*
Sample from: T. Kolotolina & A. Mekhonoshin
Mineral separation & Geochronology: U. Söderlund

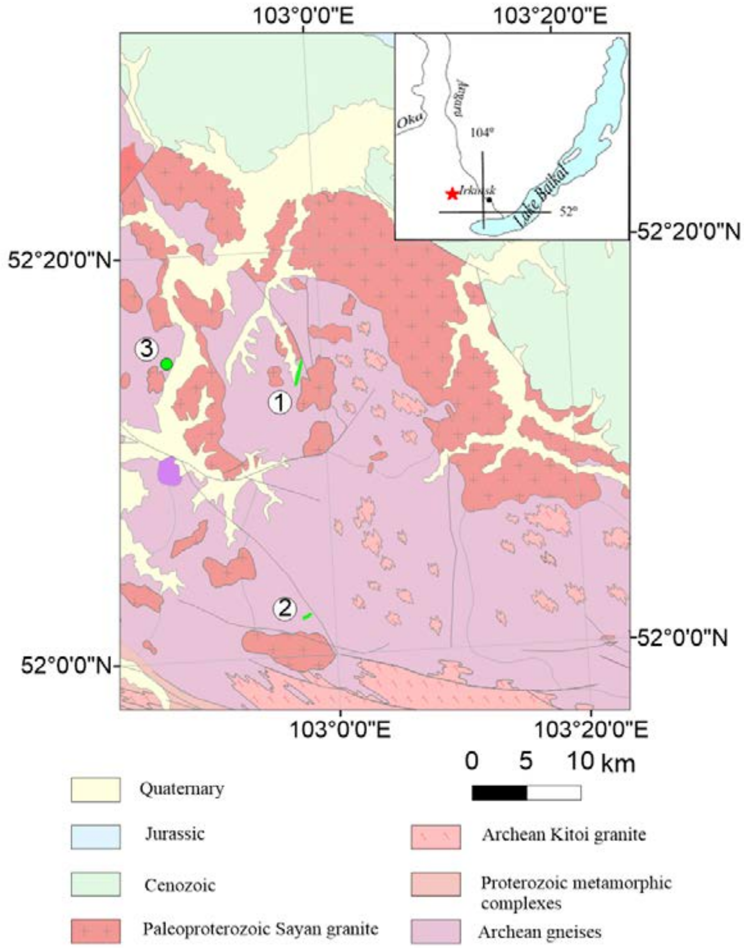

Figure S5: *Location of U-Pb dated dykes (green) cutting mainly Archean units of the Sharazhalgai block. Dykes: 1 = 200 m wide NNE-trending 1258 ± 5 Ma Ma Srednecheremshansky (this section), 2 = 150 m wide ENE-trending 1869 ± 2 Ma Malozadoisky (Section S3-7.2), 3 = 0.5 m wide ESE-trending 1864 ± 4 Ma Kitoi area dyke (Gladkochub et al. 2013; mentioned in main text). See inset map for approximate location of this region in southwestern Siberian craton.*

Sample 90-22 was collected about 15 m inside the margin of the 200 m wide NNE-trending Srednecheremshansky dyke (Fig. S5). The sample was processed at the University of Lund. Approximately 200 g of medium-grained (gabbronoritic) dolerite was crushed and finely ground using a mill tray. Baddeleyite was extracted using a water-shaking water (Wilfley) table following the procedures outlined by Söderlund and Johansson (2002), resulting in the recovery of medium-brown baddeleyite grains of a size ranging up to approximately 80 microns in the longest dimension. Three fractions of baddeleyite grains were prepared, with 2, 3 and 4 grains in each. The U- and Pb isotopic ratios were measured on a Finnigan TRITON mass spectrometer at the Swedish Museum of Natural History in Stockholm. Isotopic results are provided in Table S2 and are presented graphically in a Concordia diagram in Figure S6. Results for individual fractions overlap Concordia, and have relatively uniform $^{207}Pb/^{206}Pb$ dates. These data can be fitted to a zero-aged Pb-loss trajectory, yielding an upper intercept age of 1258 ± 5 Ma. We interpret this age to reflect the emplacement age of the gabbronorite dyke.

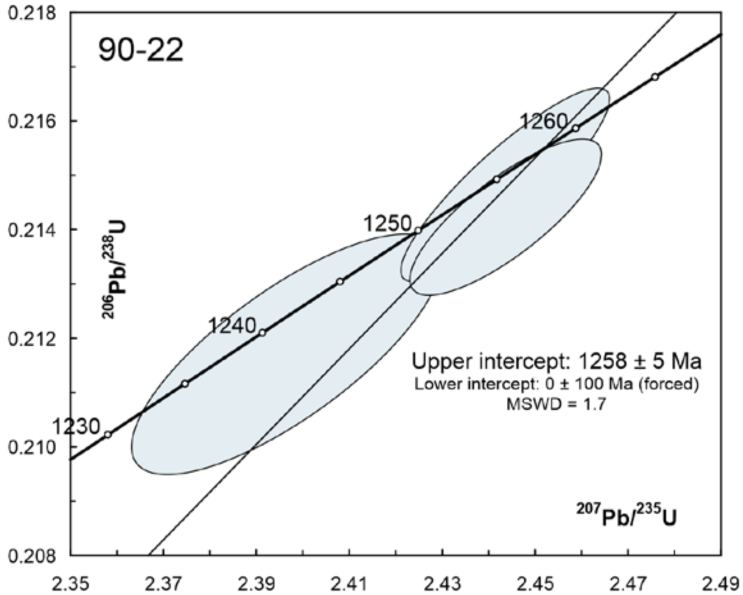

Figure S6: *Concordia diagram showing ID-TIMS baddeleyite results for sample 90-22.*

Table S2: *U-Pb TIMS data for sample 90-22*

Analysis no. (number of grains)	U/ Th	Pbc/ Pbtot[1)]	^{206}Pb/ ^{204}Pb raw[2)]	^{207}Pb/ ^{235}U [corr][3)]	± 2s % err	^{206}Pb/ ^{238}U [corr][3)]	± 2s % err	^{207}Pb/ ^{235}U [age, Ma]	^{206}Pb/ ^{238}U [age, Ma]	^{207}Pb/ ^{206}Pb [age, Ma]	± 2s	Concord-ance
Bd-1 (2 grains)	17.7	0.045	1480.2	2.4432	0.75	0.21483	0.68	1255.4	1254.5	1257.1	6.8	0.998
Bd-2 (3 grains)	14.1	0.115	532.4	2.3961	1.14	0.21169	0.86	1241.4	1237.8	1247.8	14.2	0.992
Bd-3 (4 grains)	16.7	0.039	1713.3	2.4433	0.69	0.21422	0.55	1255.5	1251.3	1262.7	8.0	0.991

1) Pbc = common Pb; Pbtot = total Pb (radiogenic + blank + initial).
2) measured ratio, corrected for fractionation and spike.
3) isotopic ratios corrected for fractionation (0.1% per amu for Pb), spike contribution, blank (1 pg Pb and 0.1 pg U), and initial common Pb. Initial common Pb corrected with isotopic compositions from the model of Stacey and Kramers (1975) at the age of the sample.

S3-4 1350 MA MAGMATISM OF SOUTHERN SIBERIA AND NORTHERN LAURENTIA

S-4.1 Listvyanka dyke, Irkutsk Promontory, southern Siberia

Sample number: *EQ01-0108*
Location: *51.84017° N, 104.8873° E*
U-Pb age: *1350 ± 6 Ma (U-Pb baddeleyite & zircon)*
Dyke trend*: N-S*
Sample from: *R.E. Ernst & E.G. Kapitonov*
Mineral separation: *M.A. Hamilton*
Geochronology: *M.A. Hamilton*

Samples of the N-S Listvyanka dykes (Fig. S7) were collected for paleomagnetism and geochemistry (in progress). The main dyke is 30 m wide and was also sampled for U-Pb dating. A small amount of both zircon and baddeleyite was recovered from sample EQ01-0108 (Fig. S8). Isotopic results from a single, chemically abraded zircon and two double-grain fractions of baddeleyite are provided in Table S3 and Fig. S8. The data are variably discordant (~1-10%) but regress with good fit to yield an upper intercept age of 1350 ± 6 Ma.

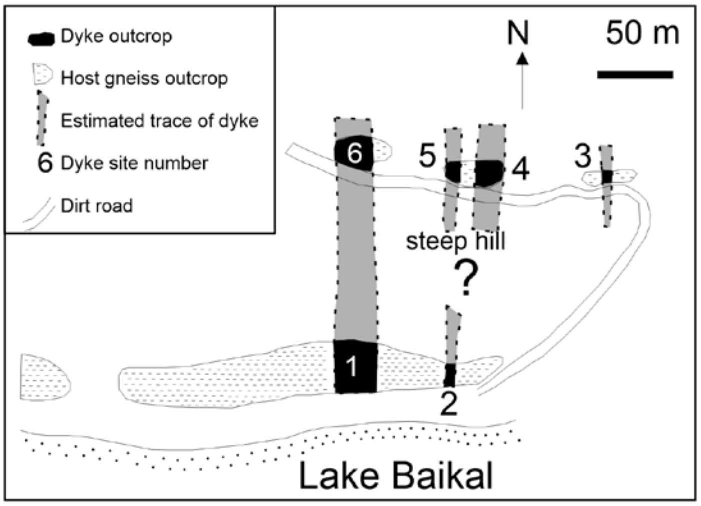

Figure S7: *Location of Site EQ01-0108 along the shore of Lake Baikal just north of the village of Listvyanka. The dated sample is from site 1 (51.84017° N, 104.8873° E).*

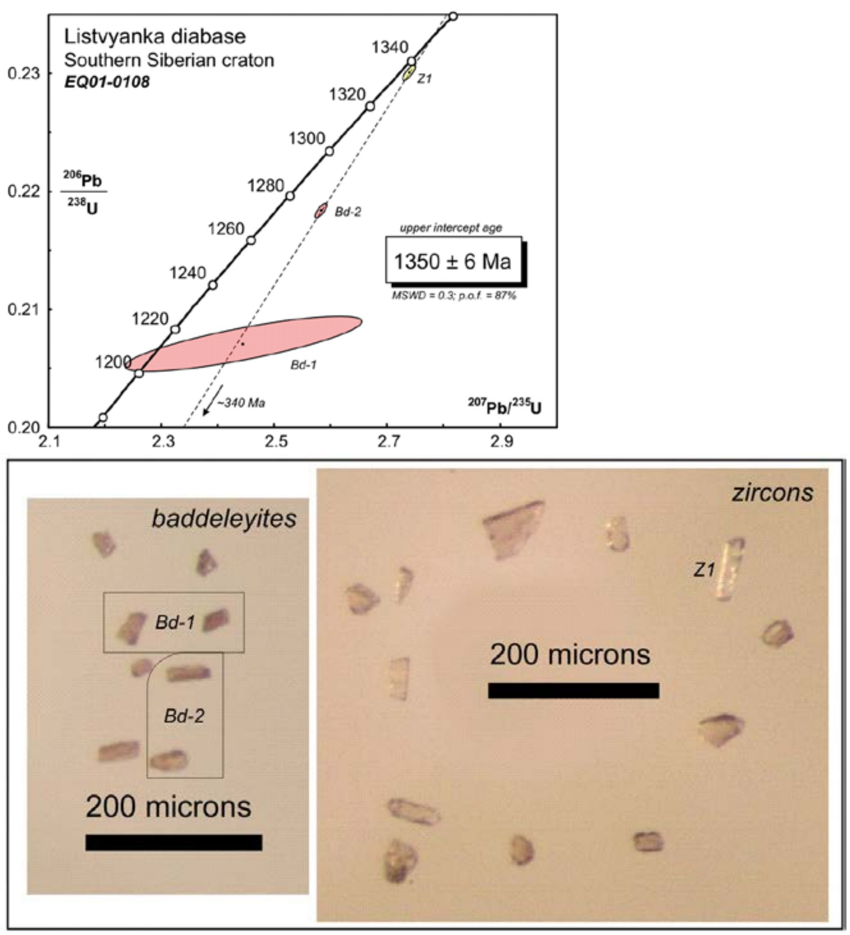

Figure S8: *U-Pb baddeleyite age for the Listvyanka dyke.*

Table S3: *ID-TIMS U-Pb baddeleyite isotopic data for Listvyanka dolerite dyke EQ01-0108.*

														Ages (Ma)						
Fraction	Description	Weight (μg)	U (ppm)	Pb^T (pg)	Pb_C (pg)	Th/U	$^{206}Pb/^{204}Pb$	$^{206}Pb/^{238}U$	± 2σ	$^{207}Pb/^{235}U$	± 2σ	$^{207}Pb/^{206}Pb$	± 2σ	$^{206}Pb/^{238}U$	± 2σ	$^{207}Pb/^{235}U$	± 2σ	$^{207}Pb/^{206}Pb$	± 2σ	Disc. (%)
EQ01-0108; Listvyanka diabase dyke, southern Siberian craton.																				
Bd-1	2 med brn bl & bl fr	0.15	189	3.28	2.28	0.144	121	0.206886	0.001954	2.44368	0.17238	0.085666	0.005435	1212.2	10.4	1255.6	51.5	1330.7	125.2	9.8
Bd-2	2 pale-med brn bl & bl fr	0.20	327	13.44	0.21	0.035	4341	0.218277	0.000543	2.58300	0.00874	0.085825	0.000169	1272.8	2.9	1295.8	2.5	1334.2	3.8	5.1
Z-1	1 cls, clr, el	0.50	189	27.51	0.38	1.290	3646	0.230045	0.000555	2.73991	0.00909	0.086382	0.000190	1334.7	2.9	1339.4	2.5	1346.7	4.3	1.0

Notes:
All analyzed fractions represent best quality, optically fresh grains of baddeleyite or zircon.
Abbreviations:cls - colourless; clr - clear; med - medium; brn - brown; bl - blade(s); fr - fragments; el - elongate.
Pb^T is total amount (in picograms) of Pb.
Pb_C is total measured common Pb (in picograms) assuming the isotopic composition of laboratory blank: 206/204 - 18.221; 207/204 - 15.612; 208/204 - 39.360 (errors of 2%).
Pb/U atomic ratios are corrected for spike, fractionation, blank, and, where necessary, initial common Pb; 206Pb/204Pb is corrected for spike and fractionation.
Th/U is model value calculated from radiogenic 208Pb/206Pb ratio and 207Pb/206Pb age, assuming concordance.
Disc. (%) - per cent discordance for the given 207Pb/206Pb age.
Uranium decay constants are from Jaffey et al. (1971).

S3-4.2 Barking Dog sill, Wellington Inlier, northern Laurentia

Sample number: *94LAAT127-2*
Location: 69.833° N, 106.875° W; (427850 E, 7748310 N, UTM zone 13)
Unit: plagioclase-phyric gabbro sill in Burnside formation
U-Pb age: 1353 ± 2 Ma U-Pb baddeleyite
Sample from: *A.N. LeCheminant*
Mineral separation: *M.A. Hamilton*
Geochronology: *M.A. Hamilton*

This distinctive plagioclase-phyric gabbro sill was emplaced within clastic sedimentary rocks of the ca. 1.9 Ga Burnside Formation, in the northern Wellington Inlier, southern Victoria Island (LeCheminant et al. 1996; Rainbird and LeCheminant 2002). This sill was distinguished from other sills and dykes in the region on the basis of stratigraphic level of intrusion (this is the lowest sill mapped in northern Wellington Inlier), mineralogy, and indications from a total chemical (electron probe) geochronology study of baddeleyite that the sill is pre-Franklin and possibly pre-Mackenzie in age. Mineralogically, the gabbro is dominated by strongly-zoned plagioclase and large, feathery pyroxenes with amphibole rims, minor quartz and K-feldspar granophyre, euhedral and skeletal ilmenite-titanomagnetite intergrowths, biotite, apatite, trace sulfides, baddeleyite, zirconolite and zircon.

A small, fresh sample, collected from a coarse- to very-coarse but non-porphyritic portion of the sill, was processed for mineral separation at the Jack Satterly Geochronology Laboratory (JSGL), University of Toronto. Sample 94LAA T127-2 yielded abundant, good quality, pale-to medium-brown baddeleyite, occurring as thin, flat broken euhedra, or as long slender thin blades, ranging up to a maximum length of ~60 microns (Fig. S9).

U-Pb analysis was carried out on three fractions, each comprising between 8-10 grains of baddeleyite. All fractions yield similar $^{207}Pb/^{206}Pb$ model ages, from 1351.7 to 1354.4 Ma, and range from 0.6 to 1.9% discordant (Table S4). Figure S9 shows a regression through the data, anchored through the origin, producing an upper intercept age of 1353 ± 2 Ma, interpreted to represent the age of emplacement and crystallization of the gabbro sill. The 1353 Ma age for this distinctive plagioclase-phyric gabbro sill represents a new and previously unrecognized age for mafic magmatism on Victoria Island. However, it has an age match in southern Siberia (Section S3-4.1 and see main text).

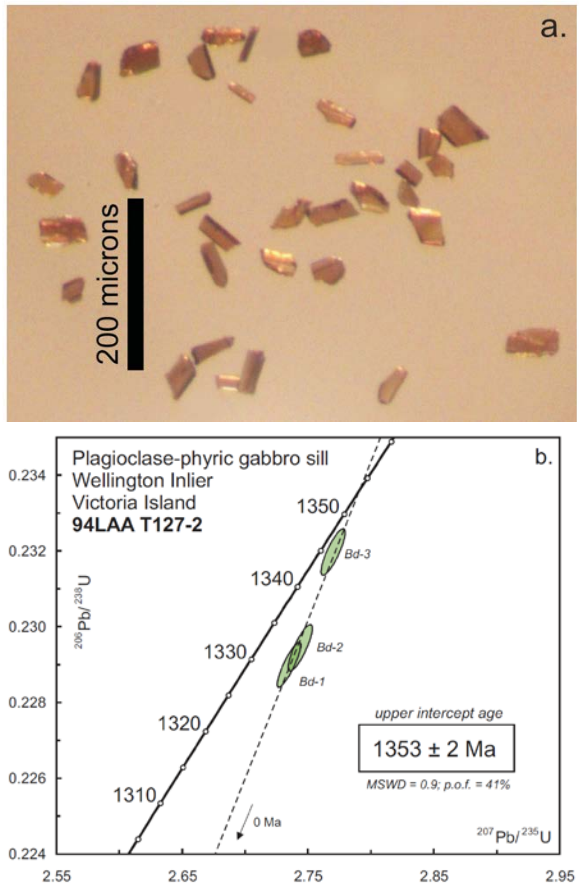

Figure S9: *U-Pb geochronology of sample 94LAAT127-2. a) Selected baddeleyite, chosen for analysis b) U-Pb Concordia diagram showing U-Pb analytical results.*

Table S4: *Baddeleyite U-Pb isotopic data for northern Wellington Inlier gabbro sill (94LAAT127-2).*

Fraction	Description	U (ppm)	Pb^T (pg)	Pb_C (pg)	Th/U	$^{206}Pb/^{204}Pb$	$^{206}Pb/^{238}U$	± 2σ	$^{207}Pb/^{235}U$	± 2σ	$^{207}Pb/^{206}Pb$	± 2σ	Ages (Ma) $^{206}Pb/^{238}U$	± 2σ	$^{207}Pb/^{235}U$	± 2σ	$^{207}Pb/^{206}Pb$	± 2σ	Disc. (%)
94LAA-T127-2 - *Plagioclase porphyritic gabbro sill, northern Wellington Inlier*																			
Bd-1	10 med brn bl & frags	144	31.06	0.36	0.034	5962	0.229017	0.000482	2.73472	0.00765	0.086605	0.000124	1329.3	2.5	1337.9	2.1	1351.7	2.8	1.83
Bd-2	10 med brn bl & frags	140	30.54	0.40	0.063	5113	0.229452	0.000494	2.74370	0.00796	0.086725	0.000141	1331.6	2.6	1340.4	2.2	1354.4	3.1	1.86
Bd-3	8 med brn bl & frags	134	30.24	0.42	0.050	5108	0.232002	0.000490	2.77103	0.00797	0.086667	0.000140	1345.0	2.6	1347.8	2.2	1353.1	3.1	0.62

Notes:

All analyzed fractions represent best quality, fresh grains of baddeleyite.

Abbreviations: med - medium; brn - brown; bl - blades; frags - fragments.

Pb^T is total amount (in picograms) of Pb.

Pb_C is total measured common Pb (in picograms) assuming the isotopic composition of laboratory blank: 206/204 - 18.221; 207/204 - 15.612; 208/204 - 39.360 (errors of 2%).

Pb/U atomic ratios are corrected for spike, fractionation, blank, and, where necessary, initial common Pb; 206Pb/204Pb is corrected for spike and fractionation.

Th/U is model value calculated from radiogenic 208Pb/206Pb ratio and 207Pb/206Pb age, assuming concordance.

Disc. (%) - per cent discordance for the given 207Pb/206Pb age.

Uranium decay constants are from Jaffey et al. (1971).

S3-5 1640 Ma U-PB AGE ON SILL FROM BIRYUSA BLOCK OF THE IRKUTSK PROMONTORY, SOUTHERN SIBERIA

S3-5.1 1640 Ma age for Biryusa block sill

Sample number: *01bi-09*
Location: *54.82478° N, 98.21164° E*
Unit: *sill in Biryusa block*
New age: *1641± 8 Ma (U-Pb baddeleyite)*
Sample from: *D.V. Metelkin*
Mineral separation: *M.A. Hamilton*
Geochronology: *M.A. Hamilton*

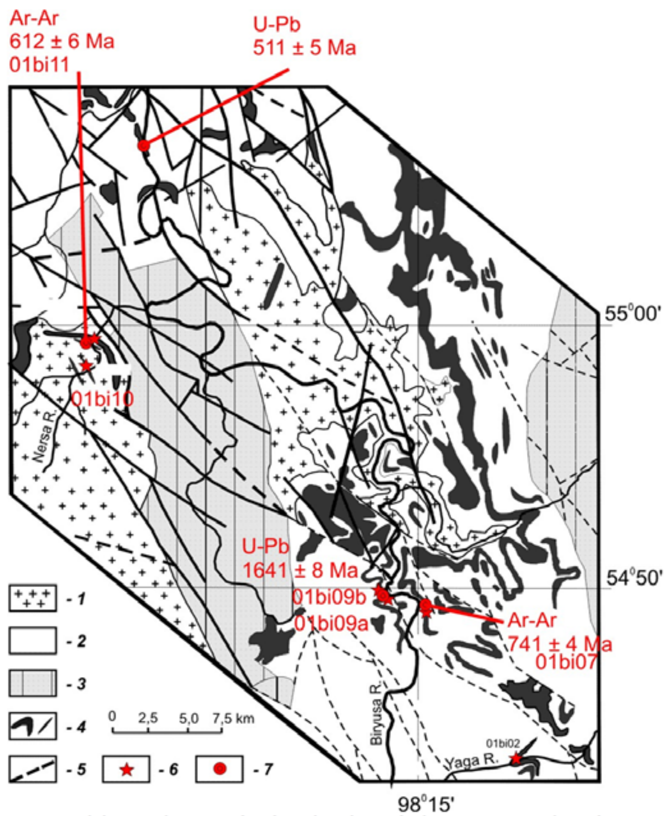

Figure S10: *Sample locations for Ar-Ar and U-Pb geochronology and paleomagnetism in southern Siberia. Location map modified after Metelkin et al. (2005). Previous geochronology after Gladkochub et al. (2006). Legend numbers are explained as follows: 1 = Paleoproterozoic granitoids of the Sayan complex; 2 = Neoproterozoic Karagas Group sedimentary rocks; 3 = Vendian Oselok Group sedimentary rocks; 4 = Neoproterozoic intrusions of the Biryusa block; 5 = major faults; 6 = paleomagnetic sites; and 7 = geochronology sites.*

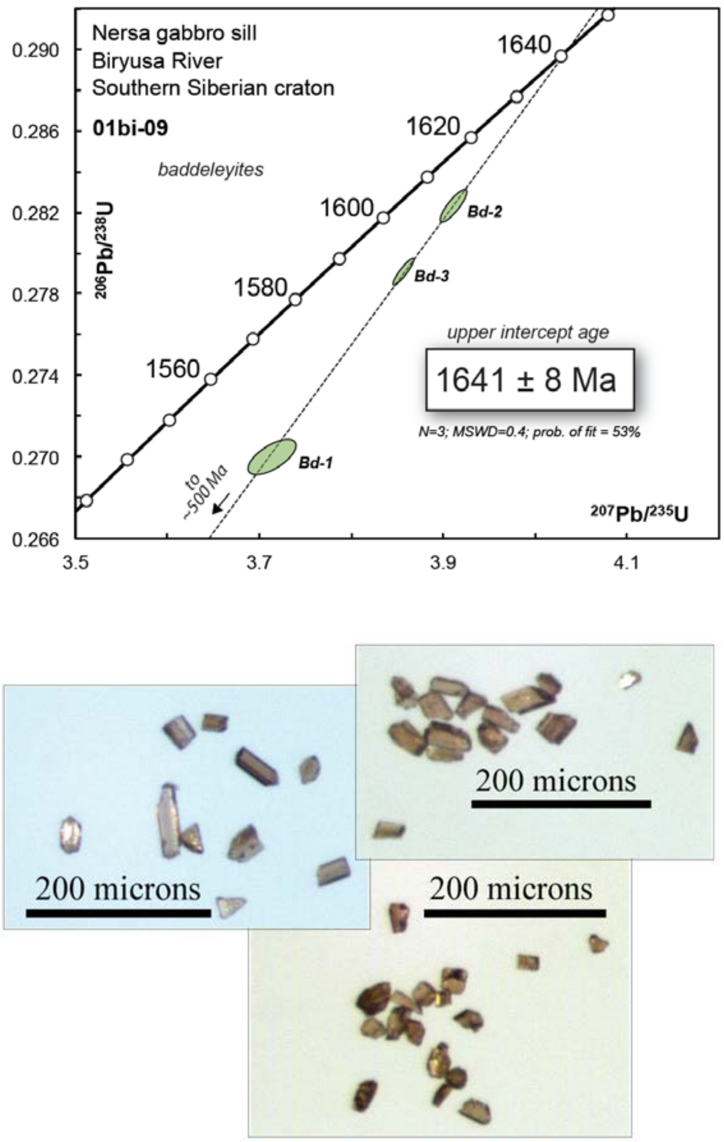

Figure S11: *U-Pb Concordia diagram and representative baddeleyites for sample 01bi-09.*

Table S5: *ID-TIMS U-Pb baddeleyite isotopic data for gabbro sill 01bi-09.*

													Ages (Ma)						
Fraction	**Description**	**Weight (μg)**	**U (ppm)**	**Pb^T (pg)**	**Pb_C (pg)**	**Th/U**	**$^{206}Pb/^{204}Pb$**	**$^{206}Pb/^{238}U$**	**± 2σ**	**$^{207}Pb/^{235}U$**	**± 2σ**	**$^{207}Pb/^{206}Pb$**	**± 2σ**	**$^{206}Pb/^{238}U$**	**± 2σ**	**$^{207}Pb/^{235}U$**	**± 2σ**	**$^{207}Pb/^{206}Pb$**	**± 2σ**	**Disc. (%)**
01BI-09, Nersa gabbro sill intruding Usmastakh Fm, Western Anabar shield.																				
Bd-1	10 pale-med brn bl & bl fr	0.15	333	17.83	0.92	0.184	1271	0.269917	0.000711	3.71238	0.02150	0.099752	0.000452	1540.4	3.6	1574.0	4.6	1619.5	8.4	5.5
Bd-2	10 med brn bl & bl fr	0.35	423	60.74	0.81	0.047	5009	0.282286	0.000666	3.91175	0.01185	0.100503	0.000163	1602.9	3.4	1616.1	2.4	1633.4	3.0	2.1
Bd-3	12 med brn bl & bl fr	0.20	382	92.31	0.82	0.059	7555	0.279043	0.000535	3.85710	0.00957	0.100251	0.000110	1586.5	2.7	1604.8	2.0	1628.7	2.0	2.9

Notes:
All analyzed fractions represent best quality, optically fresh grains of baddeleyite.
Abbreviations: med - medium; brn - brown; bl - blade(s); fr - fragments.
Pb^T is total amount (in picograms) of Pb.
Pb_C is total measured common Pb (in picograms) assuming the isotopic composition of laboratory blank: 206/204 - 18.221; 207/204 - 15.612; 208/204 - 39.360 (errors of 2%).
Pb/U atomic ratios are corrected for spike, fractionation, blank, and, where necessary, initial common Pb; 206Pb/204Pb is corrected for spike and fractionation.
Th/U is model value calculated from radiogenic 208Pb/206Pb ratio and 207Pb/206Pb age, assuming concordance.
Disc. (%) - per cent discordance for the given 207Pb/206Pb age.
Uranium decay constants are from Jaffey et al. (1971).

A gabbro sill was collected at site 01bi-09 on the west bank of Biryusa river (Fig. S10). This sample yielded a modest amount of pale- to medium-brown baddeleyite, and three multigrain fractions produced a linear array of discordant data giving an upper intercept age at 1641 Ma U-Pb (Figure S11, Table S5). This age was mentioned in Metelkin et al. (2011), but analytical details and full isotopic data and plot are presented here for the first time. This dated site is located about 2 km downstream from site 01bi07 (Fig. S10; N 54°49'29.2" E 98°12'41.9") which corresponds to a site sampled and dated by Gladkochub et al. (2006, 2007) at ca. 740 Ma (741± 4 Ma*)* using the Ar-Ar method. Previously, it was thought on the basis of paleomagnetism (e.g. Metelkin et al. 2005) that 01bi07 and 01bi09 represented parts of the same widespread ca. 740 Ma event. However, this interpretation is contradicted by our new 1641 Ma U-Pb date. There are additional complications. A dyke on the west bank of the Nersa river (01bi11) gives an Ar-Ar age of 612 Ma (Gladkochub et al. 2006). There is also a 511 Ma U-Pb age obtained from another nearby sill (Fig. S10) (Gladkochub et al. 2007). This demonstrates that there are sills of more than one age present in the area. A complete understanding of the paleomagnetic directions and Ar-Ar data (thermal overprint?) will require additional U-Pb dating combined with geochemistry to allow sills from the different events to be distinguished. Nonetheless, the 1641 Ma age reported herein is a primary age and represents a newly identified magmatic event for the Siberian craton.

S3-6 1755 MA DYKES OF THE TIMPTON RADIATING DYKE SWARM SIBERIA

Two U-Pb baddeleyite ages have been obtained from dykes belonging to the Timptano-Algamaisky dykes in the Aldan shield (Fig. S12). The 1754 and 1759 Ma U-Pb ages confirm the general accuracy of earlier Ar-Ar ages (Section S3-6.3), but carry improved precision. The Timptano-Algamaisky dykes are a subswarm of the 1750 Ma giant Timpton radiating swarm.

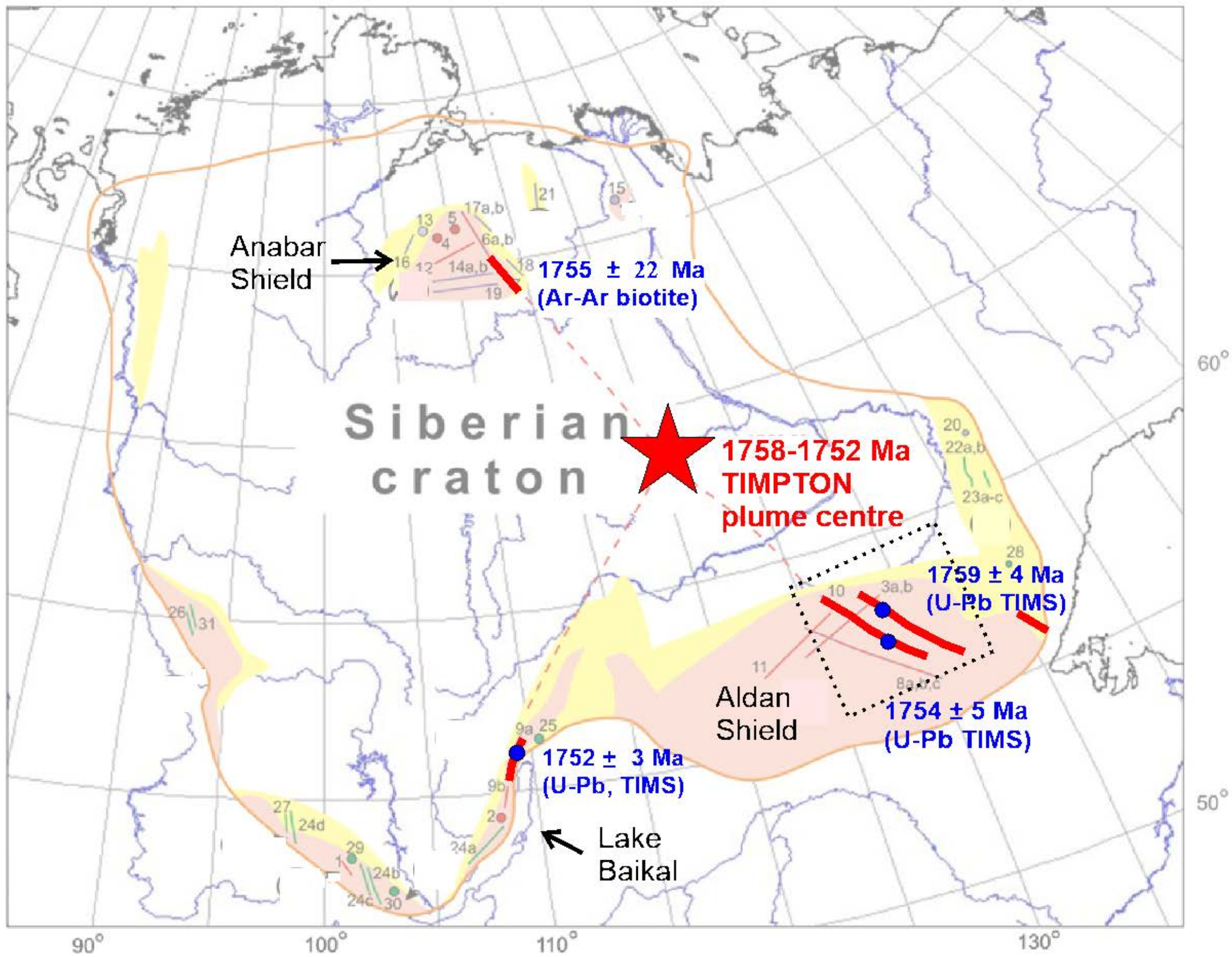

Figure S12: *Distribution of the ca. 1755 Ma Timpton radiating dyke swarm of Siberia (Ernst 2014). Dotted box shows location of Figure S13. U-Pb age of 1752 ± 3 Ma of the Lake Baikal area is from Gladkochub et al. (2010a). U-Pb ages of 1754 ± 5 and 1759 ± 4 Ma from the Aldan shield are presented below in Sections S3-6.1 and S3-6.2, respectively. The Ar-Ar age of 1755 ± 22 Ma from the Anabar shield is presented in Section S3-6.3. Basemap is from Gladkochub et al. (2010a) and the numbers on the basemap identify magmatic units discussed in that publication.*

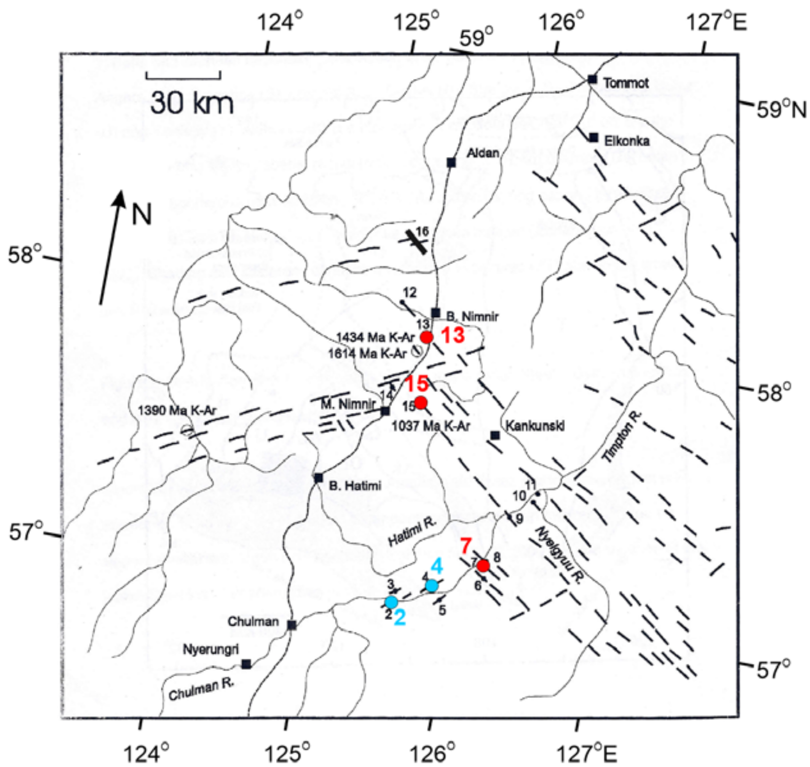

Figure S13: *Distribution of dated dykes of both the 1755 Ma Timtano-Algamaisky subswarm (red symbols) and 1870 Ma Kalaro-Nimnyrsky swarm (blue symbols). U-Pb dating (Sections S3-6.1, S3-6.2, and S3-7.1) and Ar-Ar dating (Sections S3-6.3 and S3-7.3).*

***S3-6.1 U-Pb baddeleyite age of* EQ98-0710**

Sample number*: EQ98-0710*
Location: *57.241° N, 126.137° E*
Trend and width: *NW trending, >20 m*
U-Pb age: *1754 ± 5 Ma*
Sample from: *R.E. Ernst & A.V. Okrugin*
Mineral separation & Geochronology: *U. Söderlund*

Sample EQ98-07-10 was collected at site 7 (Fig. S13) along the Timpton River from a NW-trending dyke that is a minimum of 20 m wide. Approximately 200 grams of sample EQ98-0710 was processed using the method of Söderlund and Johansson (2002), which yielded ca. 30 brown, euhedral baddeleyite grains. The best grains were split into three fractions comprising 4 to 5 grains each. The results range from 1.5 to 2.5 % discordant. An unforced regression yields intercept ages of 1757 ± 8 Ma and ca. 250 Ma, of which the latter may indicate discordance linked to the Siberian Trap event. However, we prefer to report the weighted $^{207}Pb/^{206}Pb$ age of 1754 ± 5 Ma (MSWD=2.0), equivalent to regressing the data through the origin, as the best age estimate of this sample (Fig. S14, Table S6).

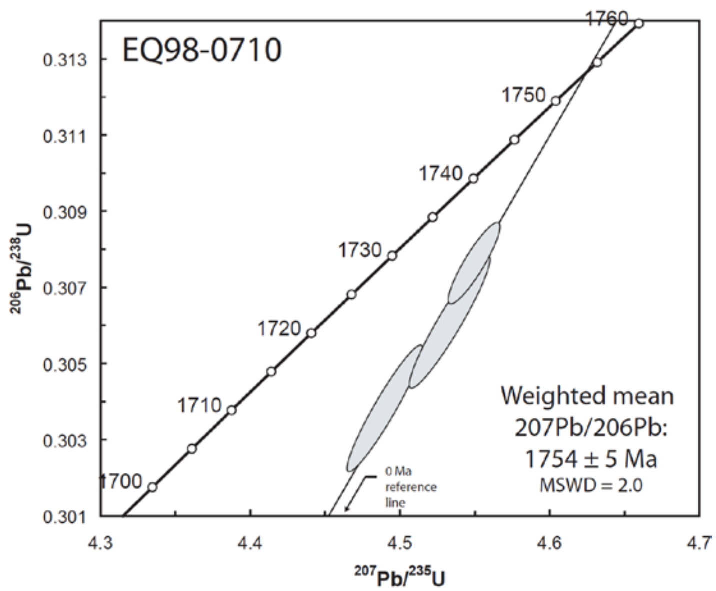

Figure S14: *Concordia diagram for U-Pb TIMS baddeleyite dating of sample EQ98-0710 (site 7 in Fig. S13). See Table* S6.

Table S6: *U-Pb TIMS data for sample EQ98-0710*

Analysis no. (number of grains)	U/ Th	Pbc/ Pbtot[1)]	^{206}Pb/ ^{204}Pb	^{207}Pb/ ^{235}U	± 2s % err	^{206}Pb/ ^{238}U	± 2s % err	^{207}Pb/ ^{235}U	^{206}Pb/ ^{238}U	^{207}Pb/ ^{206}Pb	± 2s % err	Concord-ance
			raw[2)]	[corr][3)]				[age, Ma]				
A (4 grains)	10.3	0.032	1997.1	4.4895	0.46	0.30376	0.45	1729.0	1709.9	1752.2	2.8	0.976
B (5 grains)	14.5	0.045	1407.6	4.5328	0.49	0.30605	0.47	1737.0	1721.2	1756.1	3.0	0.980
C (5 grains)	10.0	0.043	1436.0	4.5494	0.31	0.30761	0.29	1740.0	1728.9	1753.4	2.5	0.986

1) Pbc = common Pb; Pbtot = total Pb (radiogenic + blank + initial).

2) measured ratio, corrected for fractionation and spike.

3) isotopic ratios corrected for fractionation (0.1% per amu for Pb), spike contribution, blank (1 pg Pb and <1 pg U), and initial common Pb. Initial common Pb corrected with isotopic compositions from the model of Stacey and Kramers (1975) at the age of the sample

***S3-6.2 U-Pb baddeleyite age of* EQ98-1305**

Sample number: *EQ98-13-05*

Location*: 57.928° N; 125.488° E*

Dyke trend and width: *NW-trending, >20 m*

U-Pb age: *1759 ± 4 Ma*

Sample from: *R.E. Ernst & A.V. Okrugin*

Mineral separation & Geochronology: *M.A. Hamilton*

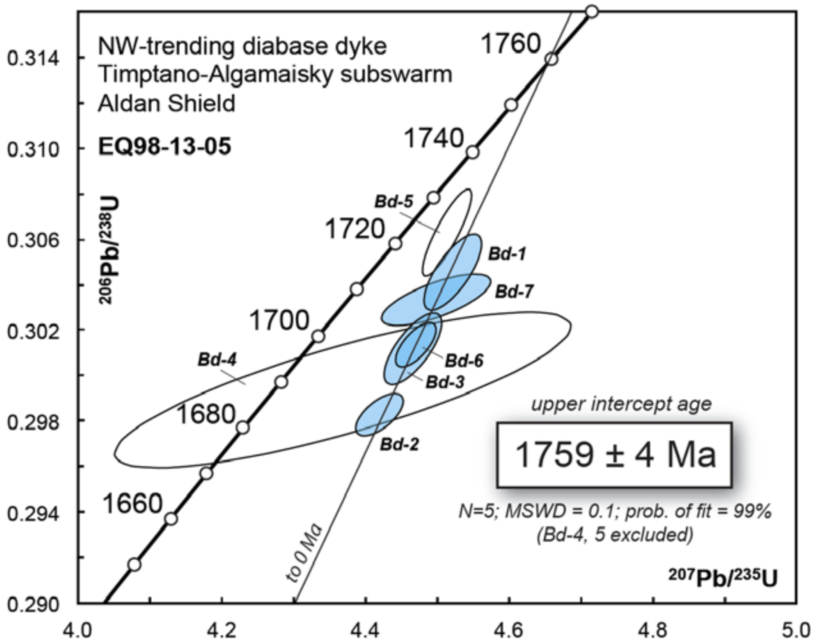

***Figure S15**: Concordia diagram for U-Pb TIMS baddeleyite dating of sample EQ98-1305 (site 13 in Fig. S13). Unshaded ellipses are fractions excluded from the regression calculation. See Table S7.*

Sample EQ98-13-05 was sampled in a road aggregate quarry, located about 1 km off the main road between the Siberian cities of Aldan and Neringry. The contacts are not fully exposed, but based on the distribution of outcrops the dyke is inferred to be approximately 20 m wide and has a NW trend.

This sample yielded a small amount of pale-medium brown baddeleyite of variable quality; approximately 60 grains were culled, from which seven fractions of crystals, ranging from 3-11 grains each, were chosen for analysis. One fraction comprised relatively dull crystals suspected to be baddeleyites with a fine microcrystalline coating of zircon (fraction Bd-2; Table S7 and Fig. S15). The data are relatively dispersed below Concordia, of which five fractions (Bd-1, -2, -3, -6 and -7) are collinear and regress to yield an upper intercept (anchored at 0 Ma) age of 1759 ± 4 Ma. We interpret this to represent the best estimate of the primary crystallization age for the dyke.

Table S7: *Baddeleyite U-Pb isotopic data for NW-trending dyke of the Aldan shield, Siberia.*

Table S7: *Baddeleyite U-Pb isotopic data for NW-trending diabase dyke of theTimptano-Algamaisky subswarm, Aldan shield, Siberia.*

Fraction	Description	U (ppm)	Pb^T (pg)	Pb_C (pg)	Th/U	$^{206}Pb/^{204}Pb$	$^{206}Pb/^{238}U$	± 2σ	$^{207}Pb/^{235}U$	± 2σ	$^{207}Pb/^{206}Pb$	± 2σ	Ages (Ma) $^{206}Pb/^{238}U$	± 2σ	$^{207}Pb/^{235}U$	± 2σ	$^{207}Pb/^{206}Pb$	± 2σ	Disc. (%)
EQ98-13-05; NW-trending mafic dyke, Aldan shield, Siberia																			
Bd-1	3 p-med br blades & frags	130	8.95	0.56	0.063	1079	0.304518	0.001371	4.52202	0.03302	0.107701	0.000538	1713.7	6.8	1735.0	6.1	1760.9	9.1	3.1
Bd-2	4 dull, med br frags; zrc frost?	276	31.20	1.37	1.717	1071	0.298219	0.000757	4.41916	0.02725	0.107474	0.000532	1682.5	3.8	1715.9	5.1	1757.0	9.1	4.8
Bd-3	6 flat, el med br blades & frags	187	8.40	0.56	0.074	1007	0.301135	0.001290	4.46606	0.03287	0.107563	0.000559	1696.9	6.4	1724.7	6.1	1758.5	9.5	4.0
Bd-4	7 flat, el med br blades & frags	111	15.61	10.72	0.132	109	0.299311	0.002810	4.36730	0.26197	0.105825	0.005588	1687.9	13.9	1706.2	50.1	1728.7	98.5	2.7
Bd-5	6 small med br blade frags	223	6.70	0.26	0.109	1704	0.306241	0.001559	4.51361	0.02836	0.106895	0.000342	1722.2	7.7	1733.5	5.2	1747.1	5.9	1.6
Bd-6	11 small med br blade frags	295	17.46	0.83	0.120	1385	0.301311	0.000796	4.46979	0.02346	0.107590	0.000425	1697.8	3.9	1725.4	4.4	1759.0	7.2	4.0
Bd-7	11 small med br blade frags	267	19.77	2.86	0.091	472	0.303283	0.000921	4.49843	0.06294	0.107575	0.001294	1707.6	4.6	1730.7	11.6	1758.7	22.1	3.3

Notes:
All analyzed fractions represent best quality, fresh grains of baddeleyite.
Abbreviations: el - elongate; p - pale; med - medium; br - brown; frag - mostly fragments of larger blades; frost- dull frosting of microcrystalline late magmatic zircon.
Pb^T is total amount (in picograms) of Pb.
Pb_C is total measured common Pb (in picograms) assuming the isotopic composition of laboratory blank: JSGL: 206/204 - 18.221; 207/204 - 15.612; 208/204 - 39.360 (errors of 2%).
Pb/U atomic ratios are corrected for spike, fractionation, blank, and, where necessary, initial common Pb; 206Pb/204Pb is corrected for spike and fractionation.
Th/U is model value calculated from radiogenic 208Pb/206Pb ratio and 207Pb/206Pb age, assuming concordance.
Disc. (%) - per cent discordance for the given 207Pb/206Pb age.
Uranium decay constants are from Jaffey et al. (1971).

S3-6.3 Ar-Ar dating of Timpton radiating dyke swarm

Sample numbers: EQ98-07-10, EQ98-15-02, EQ98-13-11 & EQ94-11
Samples from: *R.E. Ernst & A.V. Okrugin*
Ar-Ar Geochronology: *J.A. Hanes*

Ar-Ar data reported in this section provide reliable dates for two arms of the Timpton radiating dyke swarm: the SE-trending Timptano-Algamaisky subswarm and the NNW-trending Eastern Anabar subswarm. The Ar-Ar ages for the Timptano-Algamaisky correlate with U-Pb ages (Sections S3-6.1 & S3-6.2). The Ar-Ar age for the Eastern Anabar subswarm provides the key evidence linking this swarm to Timpton LIP.

1750 Ma Timptano-Algamaisky swarm, Aldan Shield (Figs. S16, S17, Table S8): Ar-Ar ages were obtained for three dykes. Sample EQ98-07-10 (from a >20 m wide dyke at site 7 in Fig. S13), yielded amphibole plateau ages of 1749 ± 7, 1748 ± 5 Ma and 1742 ± 6 Ma. Biotite plateau dates were slightly older (1767 ± 6, and 1766 ± 6 Ma), which is interpreted to reflect the presence of a small amount of excess argon in the biotite. Sample EQ98-15-02 (from a dyke at site 15 in Fig. S13) produced two amphibole and one biotite analyses. The amphibole JAH-495 has a superb plateau age of 1743 ± 09 Ma. The other amphibole analysis (JAH-349) yielded a disturbed spectrum with a plateau-segment age of 1725 ± 12 Ma. The biotite (JAH-411) spectrum gave a minimum age on a plateau-segment of 1720 ± 35 Ma. Sample EQ98-13-11 (from a 20 m wide dyke at site 13 in Fig. S13) produced an excellent biotite (JAH-414) plateau age of 1754 ± 15 Ma. The spectrum for the associated amphibole (JAH-453) is disturbed, but with mid-spectrum and late-spectrum steps that statistically overlap with the biotite age. Taken together, all these Ar-Ar ages are interpreted to indicate a ca. 1750 Ma age for the Timptano-Algamaisky swarm. This Ar-Ar age is a close match with the U-Pb ages of 1754 ± 5 Ma from site 7 (Section S3-6.1) and 1759 ± 5 Ma from site 13 (Section S3-6.2).

Ca. 1750 Ma, Eastern Anabar swarm, Anabar Shield: Of similar age is a NNW trending 30 m wide dyke of the Eastern Anabar swarm (Okrugin et al. 1990) from the Anabar shield of northern Siberia. Sample EQ94-11 (from site 11 in a 30 m wide dyke; see Fig. S13, and also Fig. 3 in Ernst et al., 2000) yielded biotite plateau ages of 1754 ± 27 Ma and 1755 ± 22 Ma (Fig. S16, Table S8).

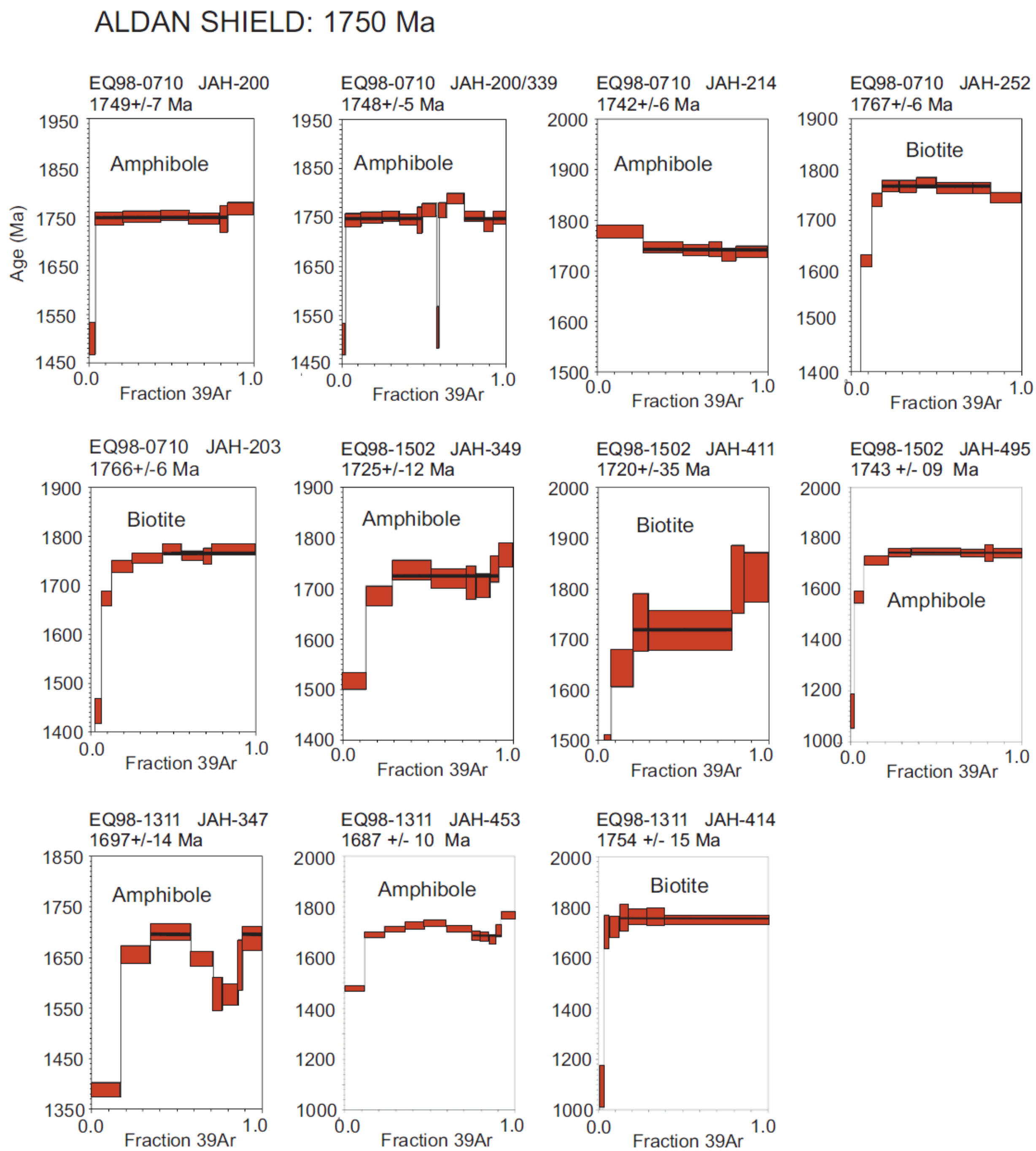

Figure S16: *Ar-Ar dating of three SE-trending dykes of the Timptano-Algamaisky sub-swarm in the Aldan shield. See Figure S13 for sample locations (sites 7, 15 and 13). Details in Table S8A.*

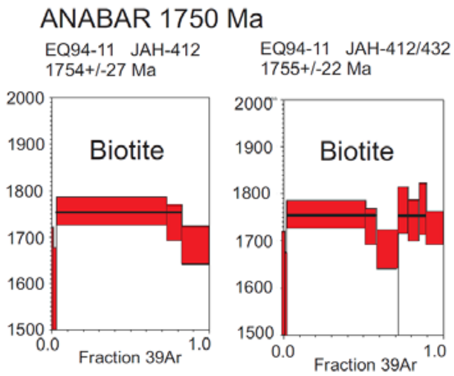

Figure S17: *Ar-Ar dating of one NNW-trending dyke of East Anabar swarm in the Anabar shield. For general location see Figure S12; for specific location see site 11 in Ernst et al. (2000). Details in Table S8B.*

Table S8: *Details on Ar-Ar dating (Parts A-C).*

A) ALDAN SHIELD ca. 1750 Ma Timptano-Algamaisky Dyke Swarm (NW-trend)

Site location on Fig. S14	**Sample Number**	**Lab Number**	**Location**	**Mineral**	**Integrated Date** (Ma)	**Plateau / Plateau-Segment Date** (Ma)
7	EQ98-0710	JAH-200	57.241°N, 126.137°E	Amphibole	1743 +/- 06	1749 ± 07
7	EQ98-0710	JAH-200/339	"	Amphibole	1747 +/- 05	1748 ± 05
7	EQ98-0710	JAH-214	"	Amphibole	1752 +/- 06	1742 ± 06
7	EQ98-0710	JAH-252	"	Biotite	1715 +/- 06	1767 ± 06
7	EQ98-0710	JAH-203	"	Biotite	1727 +/ 06	1766 ± 06
15	EQ98-1502	JAH-349	~57.7°N, ~125.4°E	Amphibole	1696 +/- 09	1725 ± 12 (*)
15	EQ98-1502	JAH-411	"	Biotite	1695 +/- 23	1720 ± 35 (*)
15	EQ98-1502	JAH-495	"	Amphibole	1718 +/- 08	1743 ± 09
13	EQ98-1311	JAH-347	57.928°N, 125.488°E	Amphibole	1614 +/ 08	1697 ± 14 (*)
13	EQ98-1311	JAH-453	"	Amphibole	1690 +/- 06	1687 ± 10 (*)
13	EQ98-1311	JAH-414	"	Biotite	1728 +/- 14	1754 ± 15

(*)=plateau segment, considered a minimum age

B) ANABAR SHIELD ca. 1750 Ma East Anabar Dyke Swarm (NW-trend)

Sample Number	**Lab Number**	**Location**	**Mineral**	**Integrated Date** (Ma)	**Plateau / Plateau-Segment Date** (Ma)
EQ94-11	JAH-412	69°59.2'N, 111°50.7'E	Biotite	1732 +/- 23	1754 ± 27
EQ94-11	JAH-412/432	"	Biotite	1734 +/- 18	1755 ± 22

C) ALDAN SHIELD ca. 1870 Ma Kalaro-Nimnyrsky Dyke Swarm (NE-trend)

Site location on Fig. S14	**Sample Number**	**Lab Number**	**Location**	**Mineral**	**Integrated Date** (Ma)	**Plateau / Plateau-Segment Date** (Ma)
4	EQ98-406	JAH-346-1	57.052°N, 125.803°E	Amphibole	1832 +/- 19	1869 ± 22
4	EQ98-406	JAH-346-2	"	Amphibole	1818 +/- 08	1866 ± 10
2	EQ98-0207	JAH-377	56.988°N, 125.484°E	Biotite	1835 +/- 10	1849 ± 11
2	EQ98-0207	JAH-375	"	Biotite	1849 +/- 21	1865 ± 22
2	EQ98-0207	JAH-460	"	Biotite	1849 +/- 07	1868 ± 08

S3-7 1870 MA KALARO-NIMNYRSKY DYKES OF SOUTHERN SIBERIA

S3-7.1 U-Pb baddeleyite age of EQ98-04-06

Sample number: *EQ98-04-06*
Location: *57.052° N, 125.803° E*
Dyke trend, dip, thickness: *ENE, subvertical, 10-20 m*
U-Pb age: *1869 ± 2 Ma (U-Pb ID-TIMS on baddeleyite)*
Sample from: *R.E. Ernst & A.V. Okrugin*
Mineral separation & Geochronology: *M.A. Hamilton*

Sample EQ98-04 was obtained from a site along the Bolshaya Kuonamka river, Anabar shield, Siberia during a 1998 expedition. The trend and width of the dyke were determined as 70^{O}E and 10-20 m.

U-Pb results for four analyzed fractions of baddeleyite, consisting of between 7-10 grains or grain fragments each, are provided in Table S9, and shown graphically in the Concordia plot Figure S18. The data are dispersed in a nearly collinear fashion, however, fraction Bd-1 shows a relatively high degree of reverse discordance and has a slightly younger $^{207}Pb/^{206}Pb$ ratio; because it is considered analytically unreliable, it is not shown in Figure S18, nor used in the age calculation. Free regression of the remaining three points yields a good fit with an upper Concordia intercept age of 1869 ± 2 Ma, and a Mesozoic lower intercept age, at ca. 140 Ma (Fig. S18).

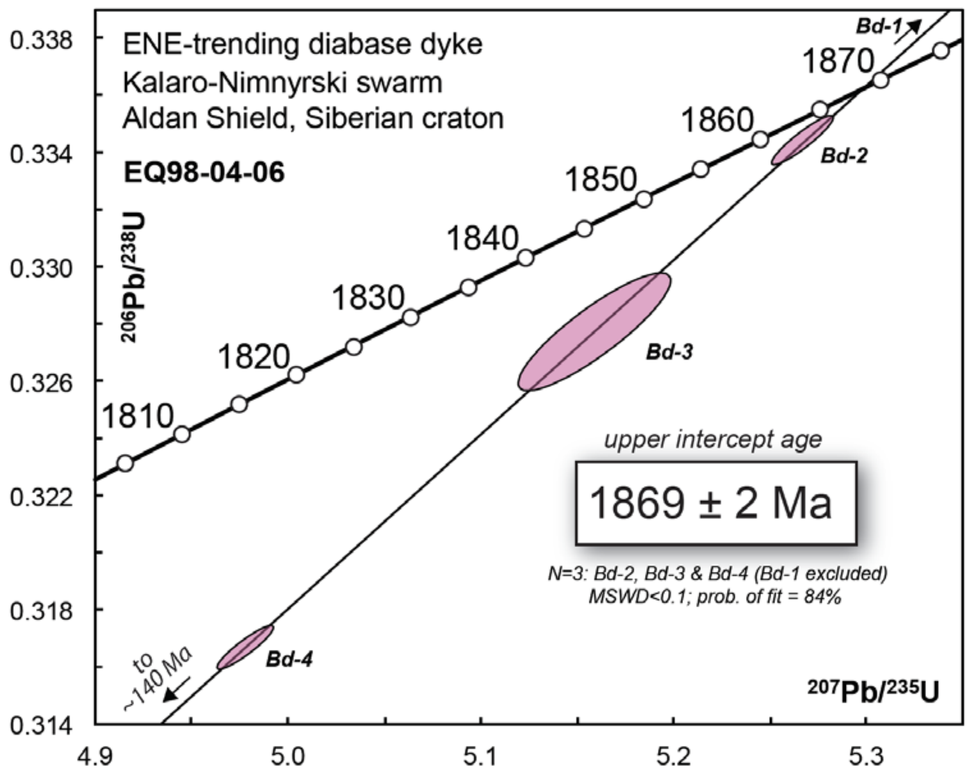

Figure S18: *Concordia U-Pb diagram for baddeleyite fractions from sample EQ98-0406. Data for fraction Bd-1 is reversely discordant, lies outside of the plot area, and is excluded from the regression shown.*

Table S9: *Baddeleyite U-Pb isotopic data for ENE-trending diabase dyke of the Kalaro-Nimnyrsky swarm, Aldan shield, Siberian craton*

Table S9. Baddeleyite U-Pb isotopic data for ENE-trending diabase dyke of the Kalaro-Nimnyrski swarm, Aldan shield, Siberian craton.

													Ages (Ma)						
Fraction	Description	U (ppm)	Pb^T (pg)	Pb_C (pg)	Th/U	$^{206}Pb/^{204}Pb$	$^{206}Pb/^{238}U$	± 2σ	$^{207}Pb/^{235}U$	± 2σ	$^{207}Pb/^{206}Pb$	± 2σ	$^{206}Pb/^{238}U$	± 2σ	$^{207}Pb/^{235}U$	± 2σ	$^{207}Pb/^{206}Pb$	± 2σ	Disc. (%)
EQ98-0406; ENE-trending mafic dyke, Aldan shield, Siberia																			
Bd-1	7 p-med br blades & frags	275	50.83	0.47	0.021	6850	0.366429	0.000756	5.74585	0.01477	0.113727	0.000127	2012.6	3.6	1938.3	2.2	1859.8	2.0	-9.6
Bd-2	8 p-med br blades & frags	124	39.97	0.30	0.028	8988	0.334417	0.000702	5.26822	0.01335	0.114255	0.000117	1859.8	3.4	1863.7	2.2	1868.2	1.8	0.5
Bd-3	9 p-med br blades & frags	294	37.16	1.52	0.023	1644	0.327683	0.001689	5.15946	0.03264	0.114196	0.000357	1827.1	8.2	1846.0	5.4	1867.2	5.6	2.5
Bd-4	10 p-med dull br blades & frags	479	89.54	0.66	0.109	8888	0.316614	0.000625	4.97642	0.01214	0.113995	0.000117	1773.2	3.1	1815.3	2.1	1864.1	1.9	5.6

Notes:
All analyzed fractions represent best quality, fresh grains of baddeleyite.
Abbreviations: el - elongate; p - pale; med - medium; br - brown; frag - mostly fragments of larger blades.
Pb^T is total amount (in picograms) of Pb.
Pb_C is total measured common Pb (in picograms) assuming the isotopic composition of laboratory blank: JSGL: 206/204 - 18.221; 207/204 - 15.612; 208/204 - 39.360 (errors of 2%).
Pb/U atomic ratios are corrected for spike, fractionation, blank, and, where necessary, initial common Pb; 206Pb/204Pb is corrected for spike and fractionation.
Th/U is model value calculated from radiogenic 208Pb/206Pb ratio and 207Pb/206Pb age, assuming concordance.
Disc. (%) - per cent discordance for the given 207Pb/206Pb age.
Uranium decay constants are from Jaffey et al. (1971).

<u>S3-7.2 U-Pb baddeleyite age of sample 93-85 from the Malozadoisky dyke</u>
Sample number: *93-85*
Location: *52.0357° N, 102.9607° E*
Dyke trend, dip, thickness: *ENE-trending, steeply dipping, ~150 m wide*
U-Pb age: *1863 ± 1 Ma (U-Pb ID-TIMS on baddeleyite)*
Sample from: *T. Kolotolina & A.S. Mekhonoshin*
Mineral separation & Geochronology: *U. Söderlund*

Sample 93-85 was collected about 15 m in from the margin of the 150 m wide NNE-trending Malozadoisky dyke (Fig. S5). Approximately 200 g of medium-grained rock was crushed and finely ground using a mill tray. Baddeleyite was extracted using a water shaking (Wilfley) table following the procedures of Söderlund and Johansson (2002), resulting in the recovery of brown baddeleyite grains ranging up to approximately 80 microns in the longest dimension. Grains are crystalline and euhedral with no trace of secondary affects such as rims of polycrystalline zircon. Three fractions of baddeleyite grains were prepared, with 4-5 grains in each. The U and Pb isotopic ratios were measured on a Finnigan TRITON mass spectrometer at the Swedish Museum of Natural History in Stockholm. Isotopic results are provided in Table S10 and are presented graphically in a Concordia diagram in Figure S19. Regression using a forced lower intercept at 0 ± 100 Ma yields an upper intercept date of 1863 ± 1 Ma (2σ), with an MSWD=1.0. Fractions plot discordant by 1-1.5% indicating minor Pb loss. Due to this low degree of discordance we interpret the upper intercept age to reflect the emplacement age of the gabbronorite Malozadoisky dyke.

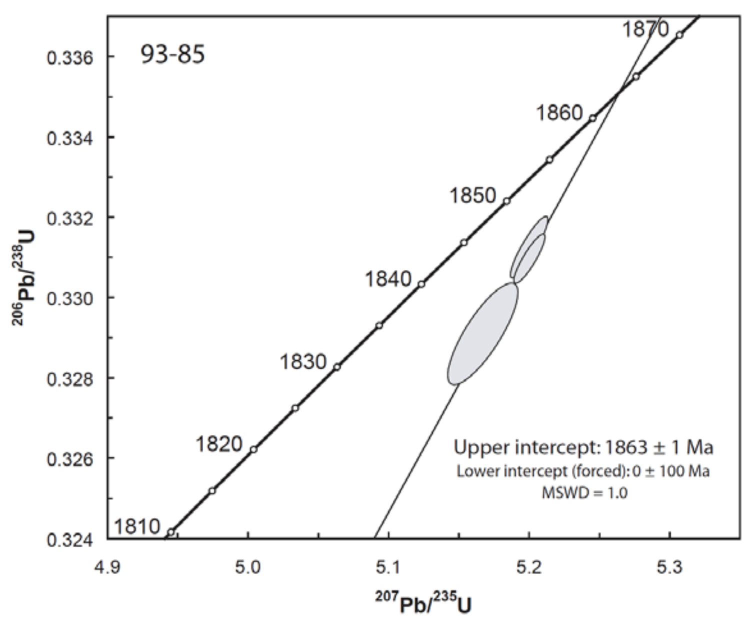

Figure S19: *Concordia diagram for sample 93-85.*

Table S10: *U-Pb TIMS data for sample 93-85.*

Analysis no. (number of grains)	U/ Th	Pbc/ Pbtot[1)]	$^{206}Pb/^{204}Pb$ raw[2)]	$^{207}Pb/^{235}U$ [corr][3)]	± 2s % err	$^{206}Pb/^{238}U$	± 2s % err	$^{207}Pb/^{235}U$ [age, Ma]	$^{206}Pb/^{238}U$	$^{207}Pb/^{206}Pb$	± 2s	Concord-ance
Bd-1 (4 grains)	5.4	0.027	2158.7	5.1677	0.40	0.32905	0.32	1847.3	1833.8	1862.6	4.2	0.985
Bd-2 (5 grains)	4.6	0.011	5507.5	5.2008	0.21	0.33122	0.19	1852.7	1844.3	1862.2	1.7	0.990
Bd-3 (4 grains)	4.4	0.007	8864.2	5.2007	0.17	0.33093	0.15	1852.7	1842.9	1863.8	1.5	0.989

[1)] Pbc = common Pb; Pbtot = total Pb (radiogenic + blank + initial).
[2)] measured ratio, corrected for fractionation and spike.
[3)] isotopic ratios corrected for fractionation (0.1% per amu for Pb), spike contribution, blank (1 pg Pb and 0.1 pg U), and initial common Pb. Initial common Pb corrected with isotopic compositions from the model of Stacey and Kramers (1975) at the age of the sample.

S3-7.3 Ar-Ar dating of Kalaro-Nimnyrsky swarm

Sample numbers: *EQ98-02-07 & EQ98-04-06*
Samples from: *R.E. Ernst & A.V. Okrugin*
Ar-Ar geochronology: *J.A. Hanes*

The Kalaro-Nimnyrsky ages, based on Ar-Ar, were only previously presented in summary form in Ernst et al. (2008). Here we present these results in more detail. Two ENE trending dykes of the Kalaro-Nimnyrsky swarm give the following Ar-Ar ages (Fig. S20, Table S8): Sample EQ98-04-06 (site 4 from a 10-20 m wide dyke; Fig. S13) yielded Ar-Ar amphibole plateau ages of 1869 ± 22 Ma, and 1866 ± 10 Ma. Sample EQ98-02-07 (site 2 from a 13 m wide dyke; Fig. S13) yielded excellent plateau ages for three biotite aliquots: 1849 ± 11 Ma, 1865 ± 22 Ma, and 1868 ± 8 Ma (this third analysis (JAH-460) being the most detailed and precise). These similar results from the two dykes are interpreted as the time of the emplacement, ca. 1870 Ma, of the Kalaro-Nimnyrsky swarm.

The U-Pb age of 1868 ± 2 Ma (Section S3-7.1) obtained from site 4 (in Fig. S13) is in excellent agreement with, and confirms, these Ar-Ar dates, and provides a robust age for the 400 km long Kalaro-Nimnyrsky swarm. This age is similar to the 1863 ± 1 Ma age for the 150 m wide Malozadoisky dyke (Section S3-7.2) which lies approximately on strike.

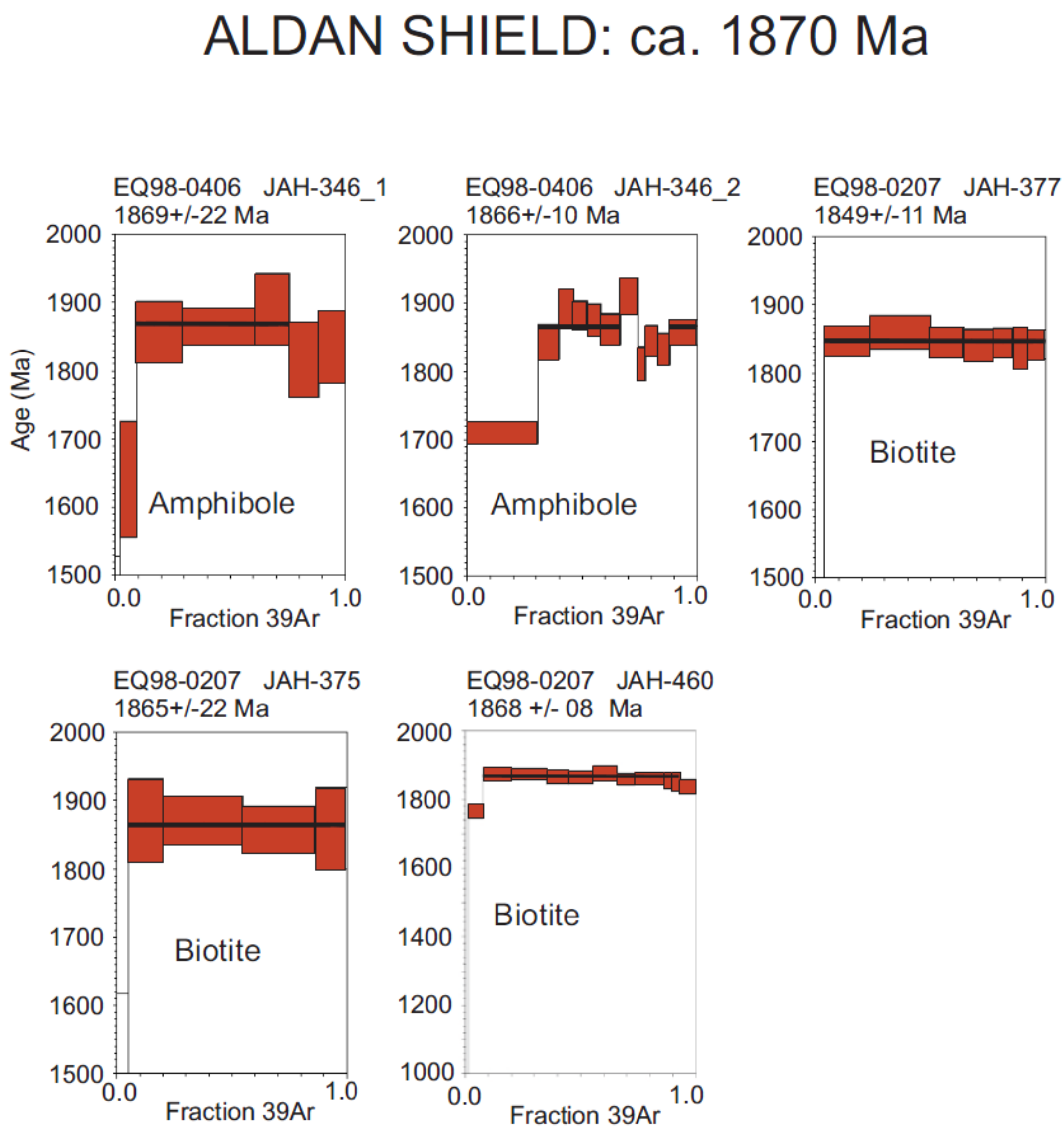

Figure S20: *Ar-Ar dating of two ENE-trending dykes in the Aldan shield. Samples EQ98-0406 and EQ98-0207 are from sites 4 and 2, respectively in Fig. S13.*

REFERENCES

Ariskin, A.A., Kostitsyn, Yu.A., Konnikov, E.G., Danyushevsky, L.V., Meffre, S., Nikolaev, G.S., McNeill, A., Kislov, E.V., Orsoev, D.A. Geochronology of the Dovyren Intrusive Complex, Northwestern Baikal Area, Russia, in the Neoproterozoic. *Geochemistry International*, **51,** 859–875 (2013).

Buchan, K.L. (2014) Reprint of "Key paleomagnetic poles and their use in Proterozoic continent and supercontinent reconstructions: A review". *Precambrian Research*, **244**, 5–22 (2014).

Buchan, K.L., Ernst, R.E., Hamilton, M.A., Mertanen, S., Pesonen, L.J., Elming, S.-Å. Rodinia: the evidence from integrated palaeomagnetism and U–Pb geochronology. *Precambrian Research*, **110**, 9–32 (2001).

Buchan, K.L., Mitchell, R.N., Wouter Bleeker, W., Hamilton, M.A., LeCheminant, A.N. Paleomagnetism of ca. 2.13–2.11 Ga Indin and ca. 1.885 Ga Ghostdyke swarms of the Slave craton: Implications for the Slave craton, APW path and relative drift of Slave, Superior and Siberian cratons in the Paleoproterozoic. *Precambrian Research*, **275**, 151-175 (2016).

Condie, K.C., Rosen, O.M., Laurentia–Siberia connection revisited. *Geology*, **22**, 168–170 (1994).

Didenko, A.N., Vodovozov, V.Y., Pisarevsky, S.A., Gladkochub, D.P., Donskaya, T.V.,Mazukabzov, A.M., Stanevich, A.M., Bibikova, E.V., Kirnozova, T.I. 2009. Palaeomagnetism andU–Pb dates of the Palaeoproterozoic Akitkan Group (South Siberia) and implications for pre-Neoproterozoic tectonics. In: Reddy, S.M., Mazumder, R., Evans,D.A.D., Collins, A.S. (Eds.), Palaeoproterozoic Supercontinents and Global Evolution. *Geological Society of London, Special Publication*, **323**, 145–163 (2009).

Didenko, A.N., Vodovozov, V.Yu., Peskov, A.Yu., Guryanov, V.A., Kosynkin, A.V. Paleomagnetism of the Ulkan massif (SE Siberian platform) and the apparent polar wander path for Siberia in late Paleoproterozoic–early Mesoproterozoic times. *Precambrian Research*, **259**, 58-77 (2015).

Eglington, B.M., Pehrsson, S.J., Ansdell, K.M., Lescuyer, J.-L., Quirt, D., Milesi, J.-P., Brown, P. A domain-based digital summary of the evolution of the Palaeoproterozoic of North America and Greenland and associated unconformity-related uranium mineralization. *Precambrian Research*, **232**, 4-26 (2013).

Ernst, R.E. Large Igneous Provinces. Cambridge University Press, 653 p. (2014).

Ernst, R.E., Jowitt, S.M. Large Igneous Provinces (LIPs) and Metallogeny. *Society of Economic Geologists Special Publication*, **17**, 17–51 (2013).

Ernst, R.E., Buchan, K.L., Hamilton, M.A., Okrugin, A.V., and Tomshin, M.D. Integrated paleomagnetism and U–Pb geochronology of mafic dikes of the eastern Anabar Shield region, Siberia: implications for Mesoproterozoic paleolatitude of Siberia and comparison with Laurentia. *The Journal of Geology*, **108,** 381–401. doi:10.1086/314413 (2000).

Ernst, R.E., Hanes, J.A., Puchkov, V.N., Okrugin, A.V., Archibald, D.A. Reconnaissance Ar–Ar dating of Proterozoic dolerite dykes and sills in Siberia and the southern Urals: identification of possible new Large Igneous Provinces (LIPs). In: Common and Regional Problems of Tectonics and Geodynamics, Moscow Tectonics Conference, GEOS, Moscow, extended abstract, p. 492-496 (2008).

Ernst, R.E., Hamilton, M.A. 725 Ma U-Pb baddeleyite age for the Dovyren mafic-ultramafic intrusion of southwestern Siberia; reconstruction with the giant 723 Ma Franklin Large Igneous Province (LIP) of northern Laurentia. In Geology of the Polar Regions of the Earth, Proceeding volume of the Annual Moscow Tectonics Conference, February 2009, volume II, p. 330-332 [In Russian] (2009).

Ernst R.E., Hamilton M.A., Soderlund U. A proposed 725 Ma Dovyren-Kingash LIP of southern Siberia, and possible reconstruction link with the 725-715 Ma Franklin LIP of northern Laurentia. Abstract Volume 35, GAC-MAC Joint Annual Meeting "Geoscience at the Edge" (May 27-29, 2012, St. John's, Newfoundland and Labrador, Canada) (2012).

Ernst, R.E., Bleeker, W., Söderlund, U., Kerr, A.C. Large Igneous Provinces and supercontinents: Toward completing the plate tectonic revolution. *Lithos*, **174**, 1–14 (2013).

Ernst, R.E., U. Söderlund, U, Hamilton, M.A., Chamberlain, K., Bleeker, W., Okrugin, A.V., LeCheminant, A.N., Kolotilina, T., Mekhonoshin, A.S., Metelkin, D., Buchan, K.L., Gladkochub, D.P., Didenko, A.N., Hanes, J.A. Long term reconstruction of southern Siberia and northern Laurentia (Slave – Rae craton) margins, based on multiple LIP barcode matches over the interval 1.9-0.7 Ga. GAC-MAC annual meeting, May 21-23, Fredericton, New Brunswick (2014).

Evans, D.A.D. The palaeomagnetically viable, long-lived and all-inclusive Rodinia supercontinent reconstruction. *Geological Society of London, Special Publication*, **327**, 371-404 (2009)

Evans, D. A. D., Mitchell, R. N. Assembly and breakup of the core of Paleoproterozoic–Mesoproterozoic supercontinent Nuna. *Geology*, **39**, 443–446 (2011).

Frost, B.R., Avchenko, O.V., Chamberlain, K.R., Frost, C.D. Evidence for extensive Proterozoic remobilization of the Aldan Shield and implications for Proterozoic plate tectonic reconstructions of Siberia and Laurentia. *Precambrian Research*, **89**, 1–23 (1998).

Gladkochub, D.P., Wingate, M.T.D., Pisarevsky, S.A., Donskaya, T.V., Mazukabzov, A.M., Ponomarchuk, V.A., Stanevich, A.M. Mafic intrusions in southwestern Siberia and implications for a Neoproterozoic connection with Laurentia. Precambrian Research, v. 147, pp. 260–278 (2006).

Gladkochub, D.P., Donskaya, T.V., Mazukabzov, A.M., Stanevich, A.M., Sklyarov, E.V, & Ponomarchuk, V.A. (2007). Signature of Precambrian extension events in the southern Siberian craton. *Russian Geology and Geophysics*, **48**, 17-31 (2007).

Gladkochub, D.P., Pisarevsky, S.A., Donskaya, T.V, Ernst, R.E., Wingate, M.T., Söderlund, U., Mazukabzov, A.M., Sklyarov, E.V., Hamilton, M.A., Hanes, J.A., (2010a). Proterozoic mafic magmatism in Siberian craton: an overview and implications for paleocontinental reconstruction. *Precambrian Research*, **183**, 660-668 (2010a).

Gladkochub, D.P., Donskaya, T.V., Wingate, M.T.D., Mazukabzov, A.M., Pisarevsky, S.A., Sklyarov, E.V., Stanevich, A.M. A one-billion-year gap in the Precambrian history of the southern Siberian Craton and the problem of the Transproterozoic supercontinent. *American Journal of Science*, **310**, 812–825 (2010b).

Gladkochub, D.P., Pisarevskii, S.A., Mazukabzov, A.M., Söderlund, U., Sklyarov, E.V., Donskaya, T.V., Ernst, R.E., Stanevich, A.M. The First Evidence of Paleoproterozoic Late-Collision Basite Magmatism in the Near-Sayan Salient of the Siberian Craton Basement, *Doklady Earth Sciences*, **450**, 583-586, doi: 10.1134/S1028334X13060019 (2013).

Hoffman, P.F. Did the breakout of Laurentia turn Gondwanaland inside out? *Science*, **252**, 1409–1412 (1991).

Hou, G-T., Santosh, M., Qian, X-L., Lister, G.S., Li, J-H. Configuration of the Late Paleoproterozoic supercontinent Columbia: Insights from radiating mafic dyke swarms *Gondwana Research* **14**, 395–409 (2008)

Jaffey, A.H., Flynn, K.F., Glendenin, L.E., Bentley, W.C., Essling, A.M. Precision measurement of half-lives and specific activities of ^{235}U and ^{238}U. *Physical Review*, **4**, 1889-1906 (1971).

LeCheminant, A.N., Rainbird, R.H., Villeneuve, M.E. Precambrian geology of northern Wellington Inlier, Victoria Island, Northwest Territories. *Geological Survey of Canada, Current Research* **1996-C**, 1-10 (1996).

Li, Z.-X., Bogdanova, S.V., Collins, A.S., Davidson, A., De Waele, B., Ernst, R.E., Fitzsimons, I.C.W., Fuck, R.A., Gladkochub, D.P., Jacobs, J., Karlstrom, K.E., Lu, S., Natapov, L.M., Pease, V., Pisarevsky, S.A., Thrane, K., Vernikovsky, V. Assembly, configuration, and break-up history of Rodinia: a synthesis. *Precambrian Research*, **160**, 179– 210 (2008).

Li. Z.X., Bogdanova, S.V.. Collins, A..S. Davidson, A., DeWaele B., Ernst R.E., Evans, D.A.D., Fitzsimons, I.C.W.. Fuck, R.A.,. Gladkochub, D.P.,. Jacobs, J. , Karlstrom, K.E., Lu, S.,. Natapov, L.M., Pease, V., Pisarevsky, S.A., Thrane, K., Vernikovsky, V. How not to build a supercontinent: A reply to J.D.A. Piper. *Precambrian Research*, **174**, 208-214 (2009).

MacLean, J.S., Sears, J.W., Chamberlain, K.R., Khudoley, A.K., Prokopiev, A.V., Kropachev, A.P., Serkina, G.G. Detrital zircon geochronologic tests of the SE Siberia-SW Laurentia paleocontinental connection. *Stephan Mueller Spec. Publ. Ser.*, **4**, 111–116, (2009)

Meert, J.G., Torsvik, T.H. Reply to JDA Piper on "The making and unmaking of a supercontinent: Rodinia revisited". *Tectonophysics*, **383**, 99-103 (2004).

Metelkin, D.V., Belonosov, I.V., Gladkochub, D.P., Donskaya, T.V., Mazukabzov, A.M. Stanevich, A.M. Paleomagnetic directions from Nersa intrusions of the Biryusa terrane, Siberian craton, as a reflection of tectonic events in the Neoproterozoic. *Russian Geology and Geophysics*, **46**, 395–410 (2005).

Metelkin, D.V., Ernst, R.E., Hamilton, M.A. A ca. 1640 Ma mafic magmatic event in southern Siberia, and links with northern Laurentia. *Geological Society of America Annual Meeting, abstract*, Minneapolis, USA (2011).

Okrugin, A.V., Oleinikov, B.V., Savvinov, V.T., Tomshin, M.D. Late Precambrian dyke swarms of the Anabar Massif, Siberian Platform, USSR. In: Parker, A.J., Rickwood, P.C., Tucker, D.H. (Eds.) Mafic Dykes and Emplacement Mechanisms. Balkema, Rotterdam, p. 529-533 (1990).

Pehrsson, S.J., Eglington, B.M., Evans, D.A.D., Huston, D., Reddy, S.M. Metallogeny and its link to orogenic style during the Nuna supercontinent cycle in Li, Z. X., Evans, D. A. D. & Murphy, J. B. (eds) Supercontinent Cycles Through Earth History. *Geological Society of London, Special Publication*, **424** (2014)

Piper, J.D.A. The Neoproterozoic Supercontinent Palaeopangaea *Gondwana Research*, **12**, 202–227 (2007).

Pisarevsky, S.A., Natapov, L.M., Donskaya, T.V., Gladkochub, D.P., Vernikovsky, V.A. Proterozoic Siberia: a promontory of Rodinia. *Precambrian Research* **160**, 66–76 (2008).

Pisarevsky, S.A. Gladkochub, D.P., Konstantinov, K.M., Mazukabzov, A.M., Stanevich, A.M., Murphy, J. B., Tait, J.A., Donskaya, T.V., Konstantinov, I.K. Paleomagnetism of Cryogenian Kitoi mafic dykes in South Siberia: Implications for Neoproterozoic paleogeography *Precambrian Research* **231**, 372–382 (2013)

Pisarevsky, S.A., Elming, S-Å., Pesonen, L.J., Li, Z-X. Mesoproterozoic paleogeography: supercontinent and beyond. *Precambrian Research* **244**, 207-225 (2014).

Polyakov, G.V., Tolstykh, N.D., Mekhonoshin, A.S., Izokh, A.E., Podlipskii, M.Yu., Orsoev, D.A., Kolotilina, T.B. Ultramafic–mafic igneous complexes of the Precambrian East Siberian metallogenic province (southern framing of the Siberian craton): age, composition, origin, and ore potential. *Russian Geology and Geophysics*, **54**, 1319–1331 (2013).

Rainbird, R.H. LeCheminant, A.N. Geology, northern Wellington Inlier, Washburn Lake area, Nunavut; Geological Survey of Canada, Open File 4263, scale 1:100 000 (2002).

Rainbird, R.H., Stern, R.A., Khudoley, A.K., Kropachev, A.P., Heaman, L.M., Sukhorukov, V.I., U–Pb geochronology of Riphean sandstone and gabbro from southeast Siberia and its bearing on the Laurentia–Siberia connection. *Earth and Planetary Science Letters*, **164**, 409–420 (1998).

Sears, J.W., Price, R.A. The Siberian connection: a case for Precambrian separation of the North American and Siberian cratons. *Geology* **6**, 267–270 (1978).

Sears, J.W., Price, R.A. Tightening the Siberian connection to western Laurentia. *Geological Society of America Bulletin*, **115**, 943–953 (2003).

Smethurst, M. A.; Khramov, A. N.; Torsvik, T. H. The Neoproterozoic and Palaeozoic palaeomagnetic data for the Siberian Platform: from Rodinia to Pangea. *Earth-Science Reviews*, **43**, 1–24 (1998)

Söderlund, U., Johansson, L. A simple way to extract baddeleyite (ZrO_2). *Geochem. Geophys. Geosyst.*, **3**(2), doi: 10.1029/2001GC000212 (2002).

Söderlund, U., Ibanez-Mejia, M., El Bahat, A., Ernst, R.E., Ikenne, M., Soulaimani, A., Youbi, N., Cousens, B., El Janati, M., Hafid, A. Reply to Comment on "U–Pb baddeleyite ages and geochemistry of dolerite dykes in the Bas-Draâ Inlier of the Anti-Atlas of Morocco: newly identified 1380 Ma event in the West African Craton" by André Michard and Dominique Gasquet. *Lithos*, **174**, 101–108 (2013).

Stacey, J.S., Kramers, J.D. Approximation of Terrestrial lead isotope evolution by a two-stage model. *Earth and Planetary Science Letters*, **26**, 207–221 (1975).

Turkina, O.M., Nozhkin, A.D., Bayanova, T.B., Dmitrieva, N.V. Isotopic Provinces and Evolution Stages of the Precambrian Crust at the Southwestern Margin of the Siberian Craton and Its Folded Framing. *Doklady Earth Sciences*, **413A**, 481–486, doi: 10.1134/S1028334X0703035X (2007).

Zhang, S-H., Li, Z-X, Evans, D.A.D., Wu, H-C., Li, H-Y, Dong, J. Pre-Rodinia supercontinent Nuna shaping up: A global synthesis with new paleomagnetic results from North China, *Earth and Planetary Science Letters*, **353-354**, 145-155 (2012).